Organometallics **2003,** *22,* 3841−3854

Pyridine− and Imidazole−Phosphinimine Bidentate Ligand Complexes: Considerations for Ethylene Oligomerization Catalysts

Liam P. Spencer, Ramadan Altwer, Pingrong Wei, Lucio Gelmini, James Gauld, and Douglas W. Stephan*

Department of Chemistry and Biochemistry, University of Windsor, Windsor, Ontario, Canada N9B 3P4

Received April 28, 2003

The series of 2-substituted diphenylphosphine pyridines **1**−**5** were synthesized and subsequently oxidized with silyl or aryl azides to give the series of pyridine−phosphinimine ligands 2-($Me_3SiNPPh_2$)C_5H_4N (**9**), 2-(2,6-$Me_2C_6H_3NPPh_2$)C_5H_4N (**10**), 2-(2,6-*i*-$Pr_2C_6H_3$-$NPPh_2$)C_5H_4N (**11**), 2-(2,6-$Me_2C_6H_3NPPh_2$)-6-MeC_5H_4N (**12**), 2-(2,6-*i*-$Pr_2C_6H_3NPPh_2$)-6-MeC_5H_4N (**13**), 2-(2,6-$Me_2C_6H_3NPPh_2$)-6-BnC_5H_4N (**14**), 2-(2,6-*i*-$Pr_2C_6H_3NPPh_2$)-6-BnC_5H_4N (**15**), 2-(2,6-$Me_2C_6H_3NPPh_2$)-6-$SiMe_3C_5H_4N$ (**16**), 2-(2,6-*i*-$Pr_2C_6H_3NPPh_2$)-6-$SiMe_3C_5H_4N$ (**17**), 2-(2,6-$Me_2C_6H_3NPPh_2$)-6-PhC_5H_4N (**18**), and 2-(2,6-*i*-$Pr_2C_6H_3NPPh_2$)-6-PhC_5H_4N (**19**). Attempts to oxidize the fluorinated phosphine 2-$P(C_6F_5)_2$-6-PhC_5H_3N (**6**) were unsuccessful. The ligand **9** reacted with $PdCl_2(PhCN)_2$ to the give the square-planar, diamagnetic compound (L)$PdCl_2$ (**20**; L = **9**), while the remaining ligands were used to prepare (L)$NiBr_2$ and (L)$FeCl_2$ complexes **21**−**30** and **31**−**40** (L = **10**-**19**), respectively. In these complexes the P atoms become part of the chelate backbone. In addition, the pyridine−phosphinimines 2-(Ph_3P=NCH_2)(C_5H_4N) (**44**), 2-(Ph_3PNCH_2)-6-Me(C_5H_3N) (**45**), and 2-(Ph_3PNCH_2)-6-Ph(C_5H_3N) (**46**) were also prepared from the reaction of 2-azidomethyl−pyridines with PPh_3. In a similar fashion the complexes (L)$PdCl_2$ (**47**, **48**; L = **44**, **45**), (L)$NiBr_2$ (**49**−**51**; L = **44**−**46**), (L)$FeCl_2$ (**52**, **53**), and (L)$CoCl_2$ (**54**, **55**; L = **44**, **45**) were prepared. In addition, the imidazole−phosphines 1-Me-2-(PPh_2)$C_3H_2N_2$ (**58**), 1-Me-2-(PPh_2)-4,5-$Ph_2C_3N_2$ (**59**), and 1-Me-2-(PPh_2)-$C_7H_6N_2$ (**60**) were prepared and oxidized to give the imidazole−phosphinimines 1-Me-2-(2,6-$Me_2C_6H_3N$=PPh_2)$C_3H_2N_2$ (**61**), 1-Me-2-(2,6-*i*-$Pr_2C_6H_3N$=PPh_2)$C_3H_2N_2$ (**62**), 1-Me-2-(2,6-$Me_2C_6H_3N$=PPh_2)-4,5-$Ph_2C_3N_2$ (**63**), 1-Me-2-(2,6-*i*-$Pr_2C_6H_3N$=PPh_2)-4,5-$Ph_2C_3N_2$ (**64**), 1-Me-2-(2,6-$Me_2C_6H_3N$=PPh_2)$C_7H_6N_2$ (**65**), 1-Me-2-(2,6-*i*-$Pr_2C_6H_3N$=PPh_2)$C_7H_6N_2$ (**66**) and 1-Me-2-(2,6-*i*-$Pr_2C_6H_3N$=PPh_2)-4-(*t*-Bu)C_3HN_2 (**67**). Subsequent complexation afforded the species (L)$PdCl_2$ (**68;** L = **61**), (L)$NiBr_2$ (**69**−**75;** L = **61**−**67**), and (L)$FeCl_2$ (**76**−**82**; L = **61**−**67**). Preliminary screening for activity as catalyst precursors for ethylene polymerization indicated that ethylene oligomerization may be occurring. In the case of complexes **30**, **40**, **74**, and **82** activation with $Et_2AlCl(ClC_6H_5)$ at 35 °C under 300 psi of ethylene effected modest catalytic dimerization of ethylene to mainly C_4 alkenes. DFT computations suggested that inclusion of P into the ligand results in diminished electrophilicity at the metal and thus a weakened ethylene−metal interaction, accounting for the modest catalytic activity. X-ray structure determinations were obtained for **2**, **20**, **26**, **27**, **35**, **37**, **40**, **49**−**51**, **54**, **68**, **79**, and **82**.

Introduction

Late-transition metal complexes have demonstrated potential as catalysts for the polymerization and oligomerization of olefins. The first industrial application of such systems was the Shell Higher Olefin Process (SHOP),[1] in which a neutral Ni catalyst containing a P−O chelating ligand effects the oligomerization of ethylene to linear C_4−C_{20} olefins. Subsequent work by Keim et al. resulted in the development of a Ni−iminophosphorane amidato ligand complex, which effected the polymerization of olefins.[2] A significant breakthrough in this area was the discovery that Ni− and Pd−diimine complexes could effect olefin polymerization catalysis with high activities at 25 °C and 1 atm using methylaluminoxane (MAO) as the catalyst activator.[3−7] Brookhart noted that the reduced steric bulk of neutral α-diimine ligands resulted in polymers with less branching and lower molecular weights.[8] The

---

* To whom correspondence should be addressed. Fax: 519-973-7098. E-mail: stephan@uwindsor.ca.

(1) Keim, W.; Kowaldt, F. H.; Goddard, R.; Krueger, C. *Angew. Chem.* **1978**, *90*, 493.

(2) Keim, W.; Appel, R.; Storeck, A.; Krueger, C.; Goddard, R. *Angew. Chem.* **1981**, *93*, 91−92.

(3) Brookhart, M.; Johnson, L. K.; Killian, C. M.; Mecking, S.; Tempel, D. J. *Polymer Prepr. (Am. Chem. Soc., Div. Polym. Chem.)* **1996**, *37*, 254−255.

(4) Brookhart, M.; Johnson, L. K.; Killian, C. M. *Abstracts of Papers*, 210th National Meeting of the American Chemical Society, Chicago, IL, Aug 20−24, 1995; American Chemical Society: Washington, DC, 1995; PMSE-252.

(5) Killian, C. M.; Tempel, D. J.; Johnson, L. K.; Brookhart, M. *J. Am. Chem. Soc.* **1996**, *118*, 11664−11665.

10.1021/om030311t CCC: $25.00
Publication on Web 08/13/2003

research groups of Brookhart[9] and Gibson[6] extended such late-metal catalysis to Fe and Co species using a bis(imino)pyridine ligand. More recently, Ni(II) complexes of N−O salicylaldiminates were shown to be very active single-component catalysts by Grubbs et al.,[10] producing highly linear polyethylene. Brookhart et al.[11] have also more recently developed a similar single-component catalyst derived from the Ni complex of 2-(2,6-diisopropylanilino)tropone. In addition, Brookhart and co-workers have shown that a cationic Ni(II)−allyl complex of a P−O chelate affords highly active catalysts in the absence of cocatalyst.[12]

A number of late-metal phosphinimine complexes[13−16] have been prepared; however, few have been examined for their potential in catalysis. For example, Bochmann et al. have reported the synthesis of group IX and X complexes of bis(aryliminophosphoranyl)ethane, bis(aryliminophosphoranyl)methane, bis(aryliminophosphoranyl)methanide, and bis(aryliminophosphoranyl)pyridine ligands.[17] The last of these complexes were structurally reminiscent of the bis(imino)pyridine ligand complexes developed by Brookhart and Gibson, although upon activation, the bis(iminophosphoranyl)pyridine complexes exhibited only modest activity. Very recently, the complex 1,2-($C_6H_4(NPPh_3)_2$)$NiCl_2$ has been reported to effect ethylene oligomerization,[18] producing C_4 and C_6 oligomers upon activation by Et_2AlCl.

We have previously developed several families of highly active Ti-containing olefin polymerization catalysts with phosphinimides as ancillary ligands.[19,20] In seeking to develop new late-metal olefin polymerization/oligomerization catalysts, we have examined several classes of chelating ligands incorporating phosphinimine donors. These phosphinimide ligands are readily prepared and derivatized, and in addition, they exhibit good thermal stability while containing a convenient ^{31}P NMR spectroscopic handle. In this paper, we describe the synthetic methods to two series of pyridine−phosphinimine ligands. In one case, the P atom is incorporated in the chelating ligand backbone, and in the other the P atom is exocyclic of the chelate ring. In addition, we describe the synthesis of imidazole−phosphinimine ligands. In each case, these ligands have been suitably substituted to provide a sterically protected pocket for the transition metal. A number of late-metal complexes have been prepared, and their utility in olefin polymerization/oligomerization has been evaluated. DFT calculations provide insights into the modest activities and future ligand design.

Experimental Section

General Data. All preparations were performed under a dry, O_2-free nitrogen atmosphere employing Schlenk line techniques, an MBraun inert-atmosphere glovebox, or a Vacuum Atmospheres Co. glovebox unless otherwise stated. Unless otherwise mentioned, all organic chemicals were reagent grade and used as received from Aldrich Chemical Co. All phosphines and metal compounds were purchased from Strem Chemical Co. and were used as received. Et_2O, EtOH, C_6H_{14}, petroleum ether (bp 35−60 °C), CH_2Cl_2, and toluene were either dried according to literature techniques or obtained directly from an Innovative Technologies solvent purification system. ^1H, $^{13}C\{^1H\}$, and $^{31}P\{^1H\}$ NMR spectra were recorded on a Bruker Avance 300 spectrometer operating at 300, 75, and 121 MHz, respectively. Several ^1H, $^{13}C\{^1H\}$, and $^{31}P\{^1H\}$ NMR spectra were recorded on a Bruker Avance 500 MHz spectrometer operating at 300, 121, and 202 MHz, respectively. Trace amounts of protonated solvents were used as references and chemical shifts reported relative to $SiMe_4$. $^{31}P\{^1H\}$ spectra were externally referenced to 85% H_3PO_4. All NMR spectra were run in C_6D_6 at 25 °C, and the $^{13}C\{^1H\}$ resonances reported are all singlets unless otherwise noted. Elemental analyses were carried out by Guelph Chemical Labs Inc., Guelph, Ontario, Canada, or the Centre for Catalysis and Materials Research (CCMR), Windsor, Ontario, Canada. In the case of the ligands **44**−**46** and **61**−**66**, elemental analysis data were not obtained; however, ^1H NMR data for these compounds have been deposited as Supporting Information. GC analysis was performed with a Shimadzu GC-9A apparatus with a Quadrex Corp. fused silica glass capillary column (methyl silicone, 25 m length, 0.25 mm i.d., and film thickness of 1.00 μm) working at 35 °C for 15 min and then heating at 25 °C min^{-1} up to 275 °C. IR spectroscopy was performed on a Bruker VECTOR 22 infrared Fourier transform spectrometer. Unpaired electron measurements were made with a Johnson Matthey magnetic susceptibility balance (Evans design). 2-Br-6-($SiMe_3$)C_5H_3N,[21] 2-Br-6-BnC_5H_3N,[22] 2-NH_2-6-PhC_5H_3N and 2-Br-6-PhC_5H_3N,[23] $PCl(C_6F_5)_2$,[24] 2-(CHO)-6-Me(C_5H_3N),[25] 2-(N_2-CH_2)-6-R(C_5H_3N)·HCl (R = Me, Ph),[26] and 2-(CHO)-6-Ph-(C_5H_3N)[27] were prepared according to literature methods. Me_3SiN_3, 2-Br-6-Me(C_5H_3N), 1-Me-$C_3H_3N_2$, $NiBr_2$(DME), 2-(PPh_2)C_3H_3N (**56**),[28] and 1-Me-2-(PPh_2)-4-(*t*-Bu)C_3HN_2 (**5**) were purchased from Aldrich Chemical Co.

---

(6) Britovsek, G. J. P.; Gibson, V.; Kimberley, B. S.; Maddox, P. J.; McTavish, S. J.; Solan, G. A.; White, A. J. P.; Williams, D. J. *Chem. Commun.* **1998**, 849−850.

(7) Abu-Surrah, A. S.; Rieger, B. *Angew. Chem., Int. Ed. Engl.* **1996**, *35*, 2475−2477.

(8) Johnson, L. K.; Killian, C. M.; Brookhart, M. *J. Am. Chem. Soc.* **1995**, *117*, 6414−6415.

(9) Small, B. L.; Brookhart, M.; Bennett, A. M. A. *J. Am. Chem. Soc.* **1998**, *120*, 4049−4050.

(10) Younkin, T. R.; Connor, E. F.; Henderson, J. I.; Friedrich, S. K.; Grubbs, R. H.; Bansleben, D. A. *Science (Washington, D.C.)* **2000**, *287*, 460−462.

(11) Hicks, F. A.; Brookhart, M. *Organometallics* **2001**, *20*, 3217−3219.

(12) Liu, W.; Malinoski, J. M.; Brookhart, M. *Organometallics* **2002**, *21*, 2836−2838.

(13) Imhoff, P.; Van Asselt, R.; Elsevier: C. J.; Zoutberg, M. C.; Stam, C. H. *Inorg. Chim. Acta* **1991**, *184*, 73−87.

(14) Imhoff, P.; Van Asselt, R.; Elsevier: C. J.; Vrieze, K.; Goubitz, K.; Van Malssen, K. F.; Stam, C. H. *Phosphorus, Sulfur Silicon Relat. Elem.* **1990**, *47*, 401−415.

(15) Dehnicke, K.; Krieger, M.; Massa, W. *Coord. Chem. Rev.* **1999**, *182*, 19−65.

(16) Avis, M. W.; Goosen, M.; Elsevier, C. J.; Veldman, N.; Kooijman, H.; Spek, A. L. *Inorg. Chim. Acta* **1997**, *264*, 43−60.

(17) Al-Benna, S.; Sarsfield, M. J.; Thornton-Pett, M.; Ormsby, D. L.; Maddox, P. J.; Bres, P.; Bochmann, M. *J. Chem. Soc., Dalton Trans.* **2000**, 4247−4257.

(18) Sauthier, M.; Leca, F.; Fernando de Souza, R.; Bernardo-Gusmao, K.; Trevisan Queiroz, L. F.; Toupet, L.; Reau, R. *New J. Chem.* **2002**, *26*, 630−635.

(19) Stephan, D. W.; Guerin, F.; Spence, R. E. v. H.; Koch, L.; Gao, X.; Brown, S. J.; Swabey, J. W.; Wang, Q.; Xu, W.; Zoricak, P.; Harrison, D. G. *Organometallics* **1999**, *18*, 2046−2048.

(20) Stephan, D. W.; Stewart, J. C.; Guerin, F.; Spence, R. E. v. H.; Xu, W.; Harrison, D. G. *Organometallics* **1999**, *18*, 1116−1118.

(21) Jutzi, P.; Lorey, O. *J. Organomet. Chem.* **1976**, *104*, 153−160.

(22) Minato, A.; Tamao, K.; Hayashi, T.; Suzuki, K.; Kumada, M. *Tetrahedron Lett.* **1980**, *21*, 845−848.

(23) Uchida, Y.; Echikawa, N.; Oae, S. *Heteroat. Chem.* **1994**, *5*, 409−413.

(24) RajanBabu, T. V.; Radetich, B.; You, K. K.; Ayers, T. A.; Casalnuovo, A. L.; Calabrese, J. C. *J. Org. Chem.* **1999**, *64*, 3429−3447.

(25) Feig, A. L.; Becker, M.; Schindler, S.; van Eldik, R.; Lippard, S. J. *Inorg. Chem.* **1996**, *35*, 2590−2601.

(26) Chuang, C.-l.; Lim, K.; Chen, Q.; Zubieta, J.; Canary, J. W. *Inorg. Chem.* **1995**, *34*, 2562−2568.

(27) Parks, J. E.; Wagner, B. E.; Holm, R. H. *Inorg. Chem.* **1971**, *10*, 2472−2478.

(28) Curtis, N. J.; Brown, R. S. *J. Org. Chem.* **1980**, *45*, 4038−4040.

Synthesis of 2-PPh$_2$C$_5$H$_4$N (1), 2-PPh$_2$-6-MeC$_5$H$_4$N (2), 2-PPh$_2$-6-BnC$_5$H$_4$N (3), 2-PPh$_2$-6-SiMe$_3$C$_5$H$_4$N (4), and 2-PPh$_2$-6-PhC$_5$H$_4$N (5). Compounds **1**−**5** were prepared using similar routes, using a modification of the literature procedure for the preparation of 2-PPh$_2$C$_5$H$_4$N; thus, only one preparation is described.[29,30] To a stirred THF solution (100 mL) of PHPh$_2$ (2.66 g, 14.3 mmol) was added n-BuLi (5.7 mL; 2.5 M in hexanes) and the deep red solution stirred overnight at 25 °C. To this solution was added dropwise a 20 mL THF solution of 2-bromopyridine (2.26 g, 14.3 mmol). After the mixture was stirred overnight, the solvent was removed in vacuo and EtOH (30 mL) was added to quench the reaction. The solvent was removed in vacuo, Et$_2$O was added (30 mL), and the solution was filtered. Removal of the ether in vacuo yielded a colorless oily solid, which was recrystallized with CH$_2$Cl$_2$ and hexane. **1**: 80% yield based on Ph$_2$PH. ^{31}P{^{1}H} NMR (δ): −3.2 (s). ^{1}H NMR (CDCl$_3$, δ): 6.49 (m, 1H, py), 6.87 (m, 1H, py), 7.04−7.09 (m, 7H, *m*-PPh$_2$, *p*-PPh$_2$, py), 7.50−7.53 (m, 4H, *o*-PPh$_2$), 8.49 (d, 1H, py). **2**: 70% yield, colorless crystals. ^{31}P{^{1}H} NMR (d_8-THF, δ): −4.0 (s). ^{1}H NMR (d_8-THF, δ): 2.48 (s, 3H, Me), 6.82 (d, 1H, 9 Hz, py), 7.11 (m, 1H, py) 7.34 (m, 10 H, PPh$_2$), 7.28 (m, 1H, py). ^{13}C{^{1}H} NMR (d_8-THF, δ): 24.4, 120.4, 124.7 (d, J_{C-P} = 3 Hz), 128.3, 128.7 (d, J_{C-P} = 19 Hz), 132.4 (d, J_{C-P} = 3 Hz), 130.2 (d, J_{C-P} = 10 Hz), 136.0, 158.5 (d, J_{C-P} = 10 Hz), 162.9 (d, J_{C-P} = 4 Hz). **3**: 65% yield, white solid. ^{31}P{^{1}H} NMR (δ): −3.2 (s). ^{1}H NMR (δ): 4.05 (s, 2H, CH$_2$), 6.67 (d, 1H, py), 6.94 (t, 1H, 9 Hz, py), 6.99 (d, 1H, 9 Hz, py), 7.17−7.23 (m, 11H, *m*-PPh$_2$, *p*-PPh$_2$, Ar), 7.59−7.63 (m, 4H, *o*-PPh$_2$). ^{13}C{^{1}H} NMR (δ): 44.1, 117.6, 123.9, 125.9 (d, J_{C-P} = 4 Hz), 126.1, 127.4, 130.6, 131.3 (d, J_{C-P} = 19 Hz), 134.1, 135.5, 136.5 (d, J_{C-P} = 10 Hz), 139.5, 158.3 (d, J_{C-P} = 10 Hz), 161.1 (d, J_{C-P} = 5 Hz). **4**: 75% yield, golden oil. The oil was purified by flash column chromatography on silica using hexanes. ^{31}P{^{1}H} NMR (δ): −3.3 (s). ^{1}H NMR (δ): 0.24 (s, 9H, SiMe$_3$), 6.95 (m, 2H, py), 7.06−7.11 (m, 7H, *m*-PPh$_2$, *p*-PPh$_2$, py), 7.55 (m, 4H, *o*-PPh$_2$). ^{13}C{^{1}H} NMR (δ): −1.9, 126.7, 127.0, 128.3 (d, J_{C-P} = 3 Hz), 128.7, 133.2 (d, J_{C-P} = 19 Hz), 134.2 (d, J_{C-P} = 19 Hz), 137.1 (d, J_{C-P} = 11 Hz), 163.2 (d, J_{C-P} = 4 Hz), 168.9 (d, J_{C-P} = 10 Hz). **5**: 65% yield, cream-colored solid. ^{31}P{^{1}H} NMR (CDCl$_3$, 25 °C, δ): −3.0 (s). ^{1}H NMR (CDCl$_3$, δ): 7.07 (m, 1H, py), 7.36−7.39 (m, 6H, *m*-PPh$_2$, Ar), 7.39−7.41 (m, 2H, *p*-PPh$_2$), 7.42 (m, 1H, py), 7.45−7.50 (m, 4H *o*-PPh$_2$), 7.63 (m, 1H, py), 7.65 (m, 1H, Ar), 8.00 (m, 2H, Ar). ^{13}C{^{1}H} NMR (CDCl$_3$, δ): 118.7, 126.4, 126.9, 128.4 (d, J_{C-P} = 4 Hz), 128.6, 128.9, 129.0, 134.3 (d, J_{C-P} = 19 Hz), 136.2 (d, J_{C-P} = 3 Hz), 136.6 (d, J_{C-P} = 11 Hz), 139.0, 157.1 (d, J_{C-P} = 12 Hz), 163.4 (d, J_{C-P} = 5 Hz).

Synthesis of 2-P(C$_6$F$_5$)$_2$-6-PhC$_5$H$_3$N (6). PhMgBr (1.0 M in THF, 1.1 mL, 1.1 mmol) was added dropwise to a stirred THF solution (10 mL) of PCl(C$_6$F$_5$)$_2$ (0.25 g, 1.1 mmol) over a period of 15 min to give a deep yellow solution. The solution was stirred overnight, with no observable change in color. A THF solution (5 mL) of PCl(C$_6$F$_5$)$_2$ (402 mg, 1.1 mmol) was then added dropwise, and the deep red solution was stirred overnight. The solvent was removed in vacuo, and the residual oil was extracted with pentane several times. The pentane extracts were cooled to −35 °C and filtered to give the white solid **8** (450 mg), which was washed several times with cold pentane. Yield: 92%. ^{31}P{^{1}H} NMR (CDCl$_3$, δ): −45.0 (quint, J_{P-F} 30 Hz). ^{1}H NMR (CDCl$_3$, δ): 7.39−7.51 (m, 2H, Ar), 7.56 (m br, 2H, Ar), 7.65 (t, J_{H-H} = 8 Hz, 1H, py), 7.69 (d, J_{H-H} 8 Hz, 1H, py), 8.00 (m, 2H, py).

Synthesis of 2,6-i-Pr$_2$C$_6$H$_3$N$_3$ (7) and 2,6-Me$_2$C$_6$H$_3$N$_3$ (8). These compounds were prepared by similar methods, using a modification of a related literature method;[31] thus, only one representative procedure is described. A mixture of 2,6-i-Pr$_2$C$_6$H$_3$NH$_2$ (10.0 g, 56.4 mmol) and NaNO$_2$ (4.3 g, 62.3 mmol) were added to a cooled (−30 °C) acidic (40 mL of concentrated HCl and 40 mL of distilled H$_2$O) solution of NaBF$_4$ (12.4 g, 112.9 mmol). After several minutes of stirring, a yellow precipitate gradually formed, which was stirred at −30 °C for 30 min. The resulting intermediate diazonium BF$_4$ salt was filtered quickly in air and washed with cold H$_2$O. This yellow sticky powder was added to a cooled (0 °C) aqueous solution (100 mL) of NaN$_3$ (11.0 g, 169.2 mmol). After vigorous gas evolution, the orange mixture was stirred overnight at 25 °C. The product was extracted from the aqueous layer with diethyl ether (3 × 30 mL) and dried with MgSO$_4$. The solution was filtered, and the solvent was removed to give a light red oil (9.5 g, 83%). The oil was not purified, due to the risk of explosion. **7**: ^{1}H NMR (CDCl$_3$, δ) 1.28 (d, J_{H-H} = 9 Hz, 12H, CHMe$_2$), 3.38 (sept, J_{H-H} = 7 Hz 2H, CHMe$_2$), 7.07−7.21 (m, 3H, C$_6$H$_3$). **8**: ^{1}H NMR (CDCl$_3$, δ) 2.21 (s, 6H, Me), 6.67 (t, J_{H-H} = 8 Hz, 1H, *p*-C$_6$H$_3$), 6.96 (d, J_{H-H} = 8 Hz, 2H, *m*-C$_6$H$_3$).

Synthesis of 2-(Me$_3$SiNPPh$_2$)C$_5$H$_4$N (9), 2-(2,6-Me$_2$C$_6$H$_3$NPPh$_2$)C$_5$H$_4$N (10), 2-(2,6-*i*-Pr$_2$C$_6$H$_3$NPPh$_2$)C$_5$H$_4$N (11), 2-(2,6-Me$_2$C$_6$H$_3$NPPh$_2$)-6-MeC$_5$H$_4$N (12), 2-(2,6-*i*-Pr$_2$C$_6$H$_3$NPPh$_2$)-6-MeC$_5$H$_4$N (13), 2-(2,6-Me$_2$C$_6$H$_3$NPPh$_2$)-6-BnC$_5$H$_4$N (14), 2-(2,6-*i*-Pr$_2$C$_6$H$_3$NPPh$_2$)-6-BnC$_5$H$_4$N (15), 2-(2,6-Me$_2$C$_6$H$_3$NPPh$_2$)-6-SiMe$_3$C$_5$H$_4$N (16), 2-(2,6-*i*-Pr$_2$C$_6$H$_3$NPPh$_2$)-6-SiMe$_3$C$_5$H$_4$N (17), 2-(2,6-Me$_2$C$_6$H$_3$NPPh$_2$)-6-PhC$_5$H$_4$N (18), and 2-(2,6-*i*-Pr$_2$C$_6$H$_3$NPPh$_2$)-6-PhC$_5$H$_4$N (19). Compounds **9**−**19** were prepared by similar methods using the appropriate phosphine and azide; thus, only one representative procedure is described. To a toluene solution (50 mL) of 2-PPh$_2$C$_5$H$_4$N (1.0 g, 3.8 mmol) was added a THF solution of Me$_3$SiN$_3$ (0.88 g, 7.6 mmol). The solution was stirred at 25 °C for several hours, and the solvent was removed to give a brown oil. Petroleum ether was added to the mixture, which was stirred for several hours and then stored at −30 °C overnight. Filtration gave a cream-colored solid, which was washed several times with hexane. **9**: 99% yield, cream-colored solid, $\nu_{P=N}$ 1350 cm^{-1}. ^{31}P{^{1}H} NMR (δ): −4.9 (s). ^{1}H NMR (CDCl$_3$, δ): 0.39 (s, 9H, −SiMe$_3$), 6.50 (m, 1H, NAr), 7.00−7.15 (m, 8H, *m*-PPh$_2$, *p*-PPh$_2$, NAr, py), 7.94−7.99 (m, 4H, *o*-PPh$_2$), 8.33 (m, 1H, py), 8.42 (m, 1H, py). ^{13}C{^{1}H} NMR (CDCl$_3$, δ): 4.8 (d, J_{C-P} = 3 Hz), 124.5 (d, J_{C-P} = 3 Hz), 128.5, 131.3 (d, J_{C-P} = 2 Hz), 133.0 (d, J_{C-P} = 10 Hz), 135.9 (d, J_{C-P} = 9 Hz), 136.1 (d, J_{C-P} = 100 Hz), 149.9 (d, J_{C-P} = 19 Hz), 159.0 (d, J_{C-P} = 135 Hz). **10**: 95% yield, cream-colored solid, $\nu_{P=N}$ 1329 cm^{-1}. ^{31}P{^{1}H} NMR (δ): −17.0 (s). ^{1}H NMR (δ): 2.42 (s, 6H, Me), 6.57−6.60 (m, 1H, py), 7.00 (t, J_{H-H} = 8 Hz, 1H, NAr), 7.09−7.12 (m, 7H, *m*-PPh$_2$, NAr, py), 7.28 (m, 2H, *p*-PPh$_2$), 8.05−8.10 (m, 4H, *o*-PPh$_2$), 8.40 (m, 1H, py), 8.45 (m, 1H, py). ^{13}C{^{1}H} NMR (CDCl$_3$, δ) 22.0, 119.1, 124.3 (d, J_{C-P} = 2.8 Hz), 127.9, 128.5, 128.7 (d, J_{C-P} = 19 Hz), 131.0 (d, J_{C-P} = 2 Hz), 132.2 (d, J_{C-P} = 8 Hz), 132.8 (d, J_{C-P} = 9 Hz), 134.8 (d, J_{C-P} = 99 Hz), 135.7 (d, J_{C-P} = 9 Hz), 147.9, 149.5 (d, J_{C-P} = 20 Hz), 158.6 (d, J_{C-P} = 137 Hz). **11**: 95% yield, cream-colored solid, $\nu_{P=N}$ 1333 cm^{-1}. ^{31}P{^{1}H} NMR (δ): −6.9 (s). ^{1}H NMR (δ): 1.14 (d, J_{H-H} = 9 Hz, 12H, CHMe$_2$), 3.66 (sept, J_{H-H} = 8 Hz, 2H, CHMe$_2$), 6.47−6.52 (m, 1H, py), 6.97−7.04 (m, 7H, *m*-PPh$_2$, NAr), 7.10 (m, 1H, py), 7.25−7.28 (m, 2H, *p*-PPh$_2$), 7.89−7.99 (m, 4H, *o*-PPh$_2$), 8.28−8.34 (m, 2H, py). ^{13}C{^{1}H} NMR (CDCl$_3$, δ): 24.4, 29.7, 120.4, 123.7, 124.7 (d, J_{C-P} = 3 Hz), 128.7, 129.2 (d, J_{C-P} = 19 Hz), 131.4 (d, J_{C-P} = 2 Hz), 133.2 (d, J_{C-P} = 9 Hz), 134.8 (d, J_{C-P} = 99 Hz), 136.0 (d, J_{C-P} = 7 Hz), 142.8 (d, J_{C-P} = 7 Hz), 144.9, 150.1 (d, J_{C-P} = 20 Hz), 158.5 (d, J_{C-P} = 139 Hz). **12**: 85% yield, cream-colored solid, $\nu_{P=N}$ 1342 cm^{-1}. ^{31}P{^{1}H} NMR (CDCl$_3$, δ): −16.5 (s). ^{1}H NMR (CDCl$_3$, δ): 2.40 (s, 6H, Me), 2.61 (s, 3H, Me), 6.62−6.65 (m, 1H, NAr), 7.00 (m, 2H, NAr), 7.09−7.12 (m, 7H, *m*-PPh$_2$, *p*-PPh$_2$, py), 7.28 (m, 2H, py), 8.05−8.10 (m, 4H, *o*-PPh$_2$). ^{13}C{^{1}H} NMR (CDCl$_3$, δ) 22.0, 25.0, 119.0, 124.1 (d, J_{C-P} = 3 Hz), 127.9, 128.1 (d, J_{C-P} = 19 Hz), 131.3 (d, J_{C-P} = 3 Hz), 132.0, 132.2, 132.8 (d, J_{C-P} = 9 Hz), 134.3 (d, J_{C-P} = 99

---

(29) Maisonnet, A.; Farr, J. P.; Olmstead, M. M.; Hunt, C. T.; Balch, A. L. *Inorg. Chem.* **1982**, *21*, 3961−3967.

(30) Newkome, G. R.; Hager, D. C. *J. Org. Chem.* **1978**, *43*, 947−949.

(31) Herring, D. L. *J. Org. Chem.* **1961**, *26*, 3998−3999.

Hz), 135.0 (d, $J_{C-P} = 9$ Hz), 147.1, 149.2 (d, $J_{C-P} = 21$ Hz), 158.4 (d, $J_{C-P} = 135$ Hz). **13**: 80% yield, cream-colored solid, $\nu_{P=N}$ 1340 cm^{-1}. ^{31}P{^{1}H} NMR (CDCl$_3$, δ): -13.6 (s). ^{1}H NMR (CDCl$_3$, δ): 1.28 (d, $J_{H-H} = 7$ Hz, 12H, CHMe$_2$), 2.55 (s, 3H, Me), 3.40 (sept, $J_{H-H} = 9$ Hz, 2H, CHMe$_2$), 6.79 (m, 1H, NAr), 6.95 (d, $J_{H-H} = 7$ Hz, 2H, NAr), 7.14 (m, 1H, py), 7.19 (m, 1H, py), 7.39 (m, 4H, *m*-PPh$_2$), 7.46 (m, 2H, *p*-PPh$_2$), 7.63 (m, 1H, py), 7.70 (m, 4H, *o*-PPh$_2$). ^{13}C{^{1}H} NMR (CDCl$_3$, δ): 24.0, 26.0, 30.2, 120.3, 123.5, 124.5 (d, $J_{C-P} = 3$ Hz), 128.5, 129.9 (d, $J_{C-P} = 19$ Hz), 131.5 (d, $J_{C-P} = 3$ Hz), 133.0, 133.6, 134.4 (d, $J_{C-P} = 99$ Hz), 135.0 (d, $J_{C-P} = 7$ Hz), 144.1, 150.5 (d, $J_{C-P} = 20$ Hz), 159.2 (d, $J_{C-P} = 139$ Hz). **14**: 88% yield, cream-colored solid, $\nu_{P=N}$ 1355 cm^{-1}. ^{31}P{^{1}H} NMR (d_8-THF, δ): -17.2 (s). ^{1}H NMR (d_8-THF, δ): 1.97 (s, 6H, Me), 4.08 (s, 2H, CH$_2$), 6.46 (t, $J_{H-H} = 8$ Hz, 1H, NAr), 6.77 (d, $J_{H-H} = 8$ Hz, 2H, NAr), 7.13−7.20 (m, 5H, CH$_2$Ph), 7.27−7.44 (m, 5H, *o*-PPh$_2$, py), 7.73 (m, 1H, py), 7.76−7.80 (m, 4H, PPh$_2$), 8.04 (t, 1H, 9.0 Hz, py). ^{13}C{^{1}H} NMR (d_8-THF, δ) 21.1, 44.1, 117.6, 123.9, 125.9 (d, $J_{C-P} = 19$ Hz), 126.1, 127.4, 127.8 (d, $J_{C-P} = 12$ Hz), 128.1, 129.0, 130.6, 131.3 (d, $J_{C-P} = 7$ Hz), 132.3 (d, $J_{C-P} = 9$ Hz), 135.5 (d, $J_{C-P} = 99$ Hz), 136.5 (d, $J_{C-P} = 9$ Hz), 139.5, 147.4, 157.4 (d, $J_{C-P} = 135$ Hz), 161.1 (d, $J_{C-P} = 20$ Hz). **15**: 85% yield, cream-colored solid, $\nu_{P=N}$ 1330 cm^{-1}. ^{31}P{^{1}H} NMR (d_8-THF, δ): -16.5 (s). ^{1}H NMR (d_8-THF, δ): 0.86 (d, $J_{H-H} = 7$ Hz, 12H, CHMe$_2$), 3.32 (sept, $J_{H-H} = 7$ Hz, 2H, CHMe$_2$), 4.08 (s, 2H, CH$_2$), 6.64 (m, 1H, NAr), 6.84 (m, 2H, NAr), 7.12−7.18 (m, 5H, CH$_2$Ph), 7.28−7.46 (m, 8H, *m*-PPh$_2$, *p*-PPh$_2$, py), 7.69−7.78 (m, 5H, *o*-PPh$_2$, py), 7.97 (m, 1H, py). ^{13}C{^{1}H} NMR (CDCl$_3$, δ): 23.1, 29.6, 45.2, 119.7, 123.2, 125.0, 127.0 (d, $J_{C-P} = 10$ Hz), 127.2 (d, $J_{C-P} = 10$ Hz), 128.9 (d, $J_{C-P} = 12$ Hz), 129.3, 130.1, 131.7, 133.5 (d, $J_{C-P} = 9$ Hz), 135.5 (d, $J_{C-P} = 100$ Hz), 137.5 (d, $J_{C-P} = 9$ Hz), 140.6, 142.8 (d, $J_{C-P} = 7$ Hz), 145.3, 157.5 (d, $J_{C-P} = 136$ Hz), 162.4 (d, $J_{C-P} = 19$ Hz). **16**: 90% yield, cream-colored solid, $\nu_{P=N}$ 1339 cm^{-1}. ^{31}P{^{1}H} NMR (δ): -16.6 (s). ^{1}H NMR (δ): 0.23 (s, 9H, $-$SiMe$_3$), 2.46 (s, 6H, Me), 7.03−7.14 (m, 9H, *m*-PPh$_2$, *p*-PPh$_2$, NAr), 7.33 (m, 1H, py), 8.04−8.13 (m, 5H, *o*-PPh$_2$, py), 8.40 (m, 1H, py). ^{13}C{^{1}H} NMR (CDCl$_3$, δ): -2.0, 20.6, 118.5, 127.3 (d, $J_{C-P} = 20$ Hz), 127.8, 127.9 (d, $J_{C-P} = 12$ Hz), 129.0 (d, $J_{C-P} = 3$ Hz), 131.0 (d, $J_{C-P} = 2$ Hz), 132.0 (d, $J_{C-P} = 17$ Hz), 132.6 (d, $J_{C-P} = 9$ Hz), 133.9 (d, $J_{C-P} = 9$ Hz), 134.0 (d, $J_{C-P} = 100$ Hz), 147.4, 157.5 (d, $J_{C-P} = 132$ Hz), 168.7 (d, $J_{C-P} = 17$ Hz). **17**: 92% yield, cream-colored solid, $\nu_{P=N}$ 1332 cm^{-1}. ^{31}P{^{1}H} NMR (CDCl$_3$, δ): -12.6 (s). ^{1}H NMR (CDCl$_3$, δ): 0.19 (s, 9H, $-$SiMe$_3$), 0.91 (d, $J_{H-H} = 9$ Hz, 12H, CHMe$_2$), 3.35 (sept, $J_{H-H} = 9$ Hz, 2H, CHMe$_2$), 6.85 (m, 1H, NAr), 6.97 (m, 2H, NAr), 7.27−7.54 (m, 7H, *m*-PPh$_2$, *p*-PPh$_2$, py), 7.69 (m, 1H, py), 7.72−7.79 (m, 4H, *o*-PPh$_2$), 7.95 (m, 1H, py). ^{13}C{^{1}H} NMR (CDCl$_3$, δ): -2.0, 23.6, 28.6, 118.9, 122.6, 127.3 (d, $J_{C-P} = 20$ Hz), 127.8 (d, $J_{C-P} = 12$ Hz), 128.8 (d, $J_{C-P} = 3$ Hz), 130.8 (d, $J_{C-P} = 2$ Hz), 132.6 (d, $J_{C-P} = 9$ Hz), 133.7 (d, $J_{C-P} = 9$ Hz), 133.9 (d,$^1J_{C-P} = 101$ Hz), 142.5 (d, $J_{C-P} = 7$ Hz), 144.2, 157.0 (d, $J_{C-P} = 132$ Hz), 168.7 (d, $J_{C-P} = 17$ Hz). **18**: 92% yield, white solid, $\nu_{P=N}$ 1342 cm^{-1}. ^{31}P{^{1}H} NMR (CDCl$_3$, δ): -11.9 (s). ^{1}H NMR (CDCl$_3$, δ): 2.07 (s, 6H, Me), 6.66 (m, 1H, NAr), 6.93 (m, 2H, NAr), 7.38−7.44 (m, 7H, *m*-PPh$_2$, Ar, py), 7.50 (m, 2H, *p*-PPh$_2$), 7.80−7.88 (m, 8H, *o*-PPh$_2$, Ar, py), 8.05 (m, 1H, py). ^{13}C{^{1}H} NMR (CDCl$_3$, δ): 21.4, 118.5, 121.0, 126.6, 126.8, 127.7, 128.0 (d, $J_{C-P} = 12$ Hz), 128.7, 129.3, 131.0, 131.1, 132.6 (d, $J_{C-P} = 9$ Hz), 133.5 (d, $J_{C-P} = 100$ Hz), 136.7 (d, $J_{C-P} = 8$ Hz), 138.4, 147.2, 156.6 (d, $J_{C-P} = 19$ Hz), 157.0 (d, $J_{C-P} = 132$ Hz). **19**: 95% yield, white solid, $\nu_{P=N}$ 1357 cm^{-1}. ^{31}P{^{1}H} NMR (CDCl$_3$, δ): -11.9 (s). ^{1}H NMR (CDCl$_3$, δ): 0.90 (d, $J_{H-H} = 7$ Hz, 2H, CHMe$_2$), 3.97 (sept, $J_{H-H} = 7$ Hz, 2H, CHMe$_2$), 6.84 (dt, 8 Hz, 2 Hz, 1H, NAr), 6.99 (dd, 8 Hz, 1 Hz, 2H, NAr), 7.37−7.43 (m, 7H, *m*-PPh$_2$, Ar, py), 7.49 (m, 2H, *p*-PPh$_2$), 7.75−7.80 (m, 4H, *o*-PPh$_2$), 7.81−7.85 (m, 4H, Ar, py), 7.91 (m, 1H, py).^{13}C{^{1}H} NMR (CDCl$_3$, δ): 22.8, 28.6, 119.1, 120.9, 122.7, 125.9, 126.6, 128.0 (d, $J_{C-P} = 11$ Hz), 128.7, 129.4, 131.1, 132.6 (d, $J_{C-P} = 7$ Hz), 133.9 (d, $J_{C-P} = 100$ Hz), 136.8 (d, $J_{C-P} = 8$ Hz), 138.4, 142.7, 144.1, 156.0 (d, $J_{C-P} = 130$ Hz), 156.7 (d, $J_{C-P} = 19$ Hz).

Synthesis of (2-(Me$_3$SiNPPh$_2$)C$_5$H$_4$N)PdCl$_2$ (20). To a toluene suspension (10 mL) of PdCl$_2$(PhCN)$_2$ (50 mg, 0.13 mmol) was added **9** (44 mg, 0.13 mmol) dissolved in 5 mL of toluene. The orange solution was stirred overnight, and the solvent volume was reduced to 3−5 mL. Et$_2$O was added to give a red precipitate, which was filtered. The solid was washed with Et$_2$O (3 × 5 mL), dried in vacuo, and recrystallized by slow diffusion of a saturated CH$_2$Cl$_2$ layer into hexane to give dark red crystals (76% yield). ^{31}P{^{1}H} NMR (CD$_2$Cl$_2$, δ): 27.9 (s). ^{1}H NMR (CD$_2$Cl$_2$, δ): 0.07 (s, 9H, SiMe$_3$), 7.36 (m, 2H, py), 7.65 (m, 4H, *m*-PPh$_2$), 7.77 (t, 2H, *p*-PPh$_2$), 7.84−7.88 (m, 4H, *o*-PPh$_2$), 8.00 (m, 2H, py), 9.30 (d, 1H, 9 Hz, py). ^{13}C{^{1}H} NMR (CD$_2$Cl$_2$, δ): 4.5 (d, $J_{C-P} = 3$ Hz), 127.3, 128.5 (d, $J_{C-P} = 121$ Hz), 128.3, 129.5 (d, $J_{C-P} = 13$ Hz), 133.8 (d, $J_{C-P} = 11$ Hz), 134.3 (d, $J_{C-P} = 2$ Hz), 138.6 (d, $J_{C-P} = 10$ Hz), 153.7 (d, $J_{C-P} = 10$ Hz), 159.0 (d, $J_{C-P} = 130$ Hz). Anal. Calcd for C$_{20}$H$_{23}$Cl$_2$N$_2$PPdSi (527.79): C, 45.51; H, 4.39; N, 5.31. Found: C, 45.02; H, 4.33; N, 5.34.

Synthesis of (L)NiBr$_2$ (21−30; L = 10−19). Compounds **21**−**30** were prepared by similar methods; thus, only one representative procedure is described. To a slight excess of **11** (1.05 equiv, 200 mg, 0.29 mmol) and NiBr$_2$(DME) (86 mg, 0.278 mmol) was added 10 mL of CH$_2$Cl$_2$. The blue suspension was stirred overnight and then was concentrated to several milliliters in vacuo. Et$_2$O (10 mL) was added, and the mixture was filtered to give a light blue powder. **21**·CH$_2$Cl$_2$: 90% yield, blue powder, $\nu_{P=N}$ 1213 cm^{-1}, $\mu_{eff} = 2.90\ \mu_B$. Anal. Calcd for C$_{26}$H$_{25}$Br$_2$Cl$_2$NiN$_2$P (685.87): C, 45.53; H, 3.67; N, 4.08. Found: C, 45.26; H, 3.59; N, 4.16. **22**: 95% yield, blue powder, $\nu_{P=N}$ 1244 cm^{-1}, $\mu_{eff} = 2.95\ \mu_B$. Anal. Calcd for C$_{29}$H$_{31}$Br$_2$NiN$_2$P (657.05): C, 53.01; H, 4.76; N, 4.26. Found: C, 53.21; H; 4.75; N, 4.21. **23**: 85% yield, light green powder, $\nu_{P=N}$ 1193 cm^{-1}, $\mu_{eff} = 3.10\ \mu_B$. Anal. Calcd for C$_{26}$H$_{25}$Br$_2$NiN$_2$P (614.97): C, 50.78; H, 4.10; N, 4.56. Found: C, 50.58; H, 4.14; N 4.96. **24**: 80% yield, light blue powder, $\nu_{P=N}$ 1242 cm^{-1}, $\mu_{eff} = 3.20\ \mu_B$. Anal. Calcd for C$_{30}$H$_{33}$Br$_2$NiN$_2$P (671.07): C, 53.69; H, 4.96; N, 4.17. Found: C, 53.57; H, 4.85; N, 4.39. **25**: 84% yield, blue powder, $\nu_{P=N}$ 1216 cm^{-1}, $\mu_{eff} = 3.15\ \mu_B$. Anal. Calcd for C$_{32}$H$_{29}$Br$_2$NiN$_2$P (691.06): C, 55.62; H, 4.23; N, 4.05. Found: C, 55.58; H, 4.52; N, 3.62. **26**: 78% yield, dark blue crystals, $\nu_{P=N}$ 1258 cm^{-1}, $\mu_{eff} = 2.97\ \mu_B$. Anal. Calcd for C$_{36}$H$_{37}$Br$_2$NiN$_2$P (747.17): C, 57.87; H, 4.99; N, 3.75. Found: C, 57.91; H, 5.27; N, 3.46. **27·CH$_2$Cl$_2$**: 75% yield, royal blue crystals, $\nu_{P=N}$ 1217 cm^{-1}, $\mu_{eff} = 3.07\ \mu_B$. Anal. Calcd for C$_{28}$H$_{31}$Br$_2$NiN$_2$PSi (673.12): C, 49.96; H, 4.64; N, 4.16. Found: C, 49.66; H, 4.92; N, 3.90. **28·0.5CH$_2$Cl$_2$**: 74% yield, blue-green powder, $\nu_{P=N}$ 1255 cm^{-1}, $\mu_{eff} = 3.23\ \mu_B$. Anal. Calcd for C$_{32}$H$_{39}$Br$_2$NiN$_2$PSi (779.71): C, 50.83; H, 5.43; N, 3.59. Found: C, 50.53; H, 5.09; N, 3.45. **29·H$_2$O**: 90% yield, purple powder, $\nu_{P=N}$ 1217 cm^{-1}, $\mu_{eff} = 2.95\ \mu_B$. Anal. Calcd for C$_{31}$H$_{27}$Br$_2$NiN$_2$P (677.03): C, 53.57; H, 4.21; N, 4.03. Found: C, 54.00; H, 4.50; N, 3.70. **30**: 92% yield, blue-green powder, $\nu_{P=N}$ 1241 cm^{-1}, $\mu_{eff} = 2.91\ \mu_B$. Anal. Calcd for C$_{35}$H$_{35}$Br$_2$NiN$_2$P (733.14): C, 57.34; H, 4.81; N, 3.82. Found: C, 57.35; H, 5.16; N, 3.58.

Synthesis of (L)FeCl$_2$ (31−40; L = 10−19). Compounds **31** to **40** were prepared by similar methods; thus, only one representative procedure is described. To a slight excess of **19** (1.05 equiv, 200 mg, 0.39 mmol) and FeCl$_2$ (47 mg, 0.37 mmol) was added 10 mL of THF. The orange suspension was stirred overnight and then was concentrated to 3−5 mL in vacuo. Et$_2$O (10 mL) was added, and the mixture was then filtered to give an orange powder. **31**: 92% yield, orange powder, $\nu_{P=N}$ 1211 cm^{-1}, $\mu_{eff} = 4.95\ \mu_B$. Anal. Calcd for C$_{25}$H$_{23}$Cl$_2$FeN$_2$P (509.19): C, 58.97; H, 4.55; N, 5.50. Found: C, 58.99; H, 4.73; N, 5.17. **32**: 87% yield, light orange solid, $\nu_{P=N}$ 1237 cm^{-1}, $\mu_{eff} = 5.04\ \mu_B$. Anal. Calcd for C$_{29}$H$_{31}$Cl$_2$FeN$_2$P (565.29): C, 61.62; H, 5.53; N, 4.96. Found: C, 61.91; H, 5.42; N, 4.86. **33**: 95% yield, dull orange solid, $\nu_{P=N}$ 1188 cm^{-1}, $\mu_{eff} = 5.12\ \mu_B$. Anal. Calcd for C$_{26}$H$_{25}$Cl$_2$FeN$_2$P (523.21): C, 59.68; H, 4.82; N, 5.35. Found: C, 59.50; H, 4.75; N, 5.55. **34**: 85% yield, orange solid, $\nu_{P=N}$ 1242 cm^{-1}, $\mu_{eff} = 5.24\ \mu_B$. Anal. Calcd for C$_{30}$H$_{33}$Cl$_2$FeN$_2$P

(579.32): C, 62.20; H, 5.74; N, 4.84. Found: C, 62.32; H, 5.93; N, 4.50. **35**·CH_2Cl_2: 67% yield, deep orange crystals, $\nu_{P=N}$ 1215 cm^{-1}, $\mu_{eff} = 5.14\ \mu_B$. Anal. Calcd for $C_{33}H_{31}Cl_4FeN_2P$ (684.24): C, 57.93; H, 4.57; N, 4.09. Found: C, 57.47; H, 5.14; N, 3.86. **36**·CH_2Cl_2: 76% yield, orange crystals, $\nu_{P=N}$ 1258 cm^{-1}, $\mu_{eff} = 5.20\ \mu_B$. Anal. Calcd for $C_{37}H_{39}Cl_4FeN_2P$ (740.35): C, 60.03; H, 5.31; N, 3.78. Found: C, 59.82; H, 5.61; N, 3.39. **37**: 76% yield, orange-red crystals, $\nu_{P=N}$ 1213 cm^{-1}, $\mu_{eff} = 5.07\ \mu_B$. Anal. Calcd for $C_{28}H_{31}Cl_2FeN_2PSi$ (581.37): C, 57.85; H, 5.37; N, 4.82. Found: C, 57.86; H, 5.45; N, 4.84. **38**: 72% yield, orange crystals, $\nu_{P=N}$ 1254 cm^{-1}, $\mu_{eff} = 4.99\ \mu_B$. Anal. Calcd for $C_{32}H_{39}Cl_2FeN_2PSi$ (637.48): C, 60.29; H, 6.17; N, 4.39. Found: C, 60.07; H, 6.15; N, 4.12. **39**·H_2O: 55% yield, dark orange crystals, $\nu_{P=N}$ 1242 cm^{-1}, $\mu_{eff} = 5.35\ \mu_B$. Anal. Calcd for $C_{31}H_{29}Cl_2FeN_2OP$ (603.30): C, 61.72; H, 4.85; N, 4.64. Found: C, 61.60; H, 5.08; N, 4.19. **40**·H_2O: 65% yield, dark orange crystals, $\nu_{P=N}$ 1217 cm^{-1}, $\mu_{eff} = 5.19\ \mu_B$. Anal. Calcd for $C_{35}H_{37}Cl_2FeN_2OP$ (659.41): C, 63.75; H, 5.66; N, 4.25. Found: C, 63.69; H, 5.68; N, 4.13.

Synthesis of 2-(N_3CH_2)(C_5H_4N) (41), 2-(N_3CH_2)-6-Me-(C_5H_3N) (42), 2-(N_3CH_2)-6-Ph(C_5H_3N) (43). To a stirred solution of 2-($ClCH_2$)(C_5H_4N)·HCl (18.28 mmol, 3.00 g) in 100 mL of H_2O was added 21.9 mmol (1.426 g) of NaN_3. The stirred mixture was refluxed for 2 days and then cooled, and the solution was neutralized with $NaHCO_3$. The product was extracted into CH_2Cl_2, and the organic layer was dried over anhydrous $MgSO_4$. After filtration the solvent was removed under vacuum to give the brown oil **41** (70%). The oil was not purified due to the risk of explosion. ^{1}H NMR (δ): 8.45 (d, $J_{H-H} = 3$ Hz, 1H, py), 7.25 (d, $J_{H-H} = 1$ Hz, 1H, py), 7.09−7.06 (m, 1H, py), 6.98 (t, $J_{H-H} = 3$ Hz, 1H, py), 4.08 (s, 2H, CH_2). ^{13}C{^{1}H} NMR (CD_2Cl_2, δ): 156.8, 150.2, 136.6, 128.7 (d, $J_{C-P} = 99$ Hz), 122.9, 122.0, 55.0. **42**: 85% yield, brown oil. ^{1}H NMR ($CDCl_3$, δ): 7.58 (d, $J_{H-H} = 12$ Hz, 1H, py), 7.13 (t, $J_{H-H} = 3$ Hz, 1H, py), 7.09 (d, $J_{H-H} = 3$ Hz, 1H, py), 4.43 (s, 2H, CH_2), 2.55 (s, 3H, Me). ^{13}C{^{1}H} NMR (CD_2Cl_2, δ): 158.2, 149.2, 136.1, 120.0 (d, $J_{C-P} = 8$ Hz), 122.9, 122.0, 56.0, 21.2. **43**: 80% yield, light brown oil. ^{1}H NMR ($CDCl_3$, δ): δ 8.02 (d, $J_{H-H} = 3$ Hz, 3H, Ar), 7.54−7. 37 (m, 2H, Ar), 7.5−7.3 (m, 1H, py), 7.08 (t, $J_{H-H} = 6$ Hz, 1H, py), 6.87 (d, $J_{H-H} = 1$ Hz, 1H, py), 4.52 (s, 2H, CH_2). ^{13}C{^{1}H} NMR (CD_2Cl_2, δ): 156.8, 157.0, 139.7, 137.1, 129, 127 (t, $J_{C-P} = 44$ Hz), 119.4 (d, $J_{C-P} = 2$ Hz), 56.0.

Synthesis of 2-(Ph_3PNCH_2)C_5H_4N (44), 2-(Ph_3PNCH_2)-6-MeC_5H_3N (45), 2-(Ph_3PNCH_2)-6-PhC_5H_3N (46). To a stirred solution of **41** (7.40 mmol, 1.00 g) in toluene (50 mL) under N_2 was added PPh_3 (3.70 mmol, 0.97 g). The mixture was heated for 6 h and cooled and then the solvent removed under vacuum to give a yellow powder of **44**: 86% yield, white solid, $\nu_{P=N}$ 1360 cm^{-1}. ^{31}P NMR (δ): 7.8 (s). ^{1}H NMR (δ): 8.48 (d, $J_{H-H} = 9$ Hz, 1H, py), 7.86−7.80 (m, 11H, Ar), 7.78 (d, $J_{H-H} = 6$ Hz, 4H, Ar), 7.25 (d, $J_{H-H} = 1$ Hz, 1H, py), 7.16 (t, $J_{H-H} = 3$ Hz, 1H, py), 7.14−7.01 (m, 1H, py), 5.09 (s, 2H, CH_2). ^{13}C{^{1}H} NMR (CD_2Cl_2, δ): 156.8, 149.4, 135.9, 123.7, 128.0 (d, $J_{C-P} = 150$ Hz) ,121.9, 122.0, 42.0. **45**: 80% yield, white solid, $\nu_{P=N}$ 1358 cm^{-1}. ^{31}P{^{1}H} NMR (δ): 7.8 (s). ^{1}H NMR (δ): 8.66 (d, 2H, Ar), 8.57 (d, $J_{H-H} = 42$ Hz, 2H, Ar), 7.85−7.80 (m, 11H, Ar), 7.50−7.44 (d, $J_{H-H} = 18$ Hz, 1H, py), 7.25−7.09 (m, 1H, py), 7.08 (t, $J_{H-H} = 6$ Hz, 1H, py), 5.10 (s, 2H, CH_2), 2.54 (s, 3H, Me). ^{13}C{^{1}H} NMR (CD_2Cl_2): δ 158.2, 136.1, 128.1 (d, $J_{C-P} = 90$ Hz), 48.8, 21.2. **46**: 55% yield, yellow solid, $\nu_{P=N}$ 1355 cm^{-1}. ^{31}P NMR (δ): 7.9 (s). ^{1}H NMR (δ): 7.76−7.72 (m, 11H, Ph), 7.54 (t, $J_{H-H} = 3$ Hz, 4H, Ph). 7.99 (d, $J_{H-H} = 1$ Hz, 2H, Ar), 7.35 (d, $J_{H-H} = 2$ Hz, 2H, Ar), 7.28 (s, 1H, Ar), 7.38 (s, 1H, py), 7.46 (d, $J_{H-H} = 1$ Hz, 1H, py), 7.44 (d, $J_{H-H} = 1$ Hz,-1H, py), 5.34 (s, 2H, CH_2). ^{13}C{^{1}H} NMR (CD_2Cl_2, δ): 158.8, 157.0, 137.1, 129.0, 128.0 (d, $J_{C-P} = 159$ Hz), 127.1, 119.4, 48.8.

Synthesis of (L)$PdCl_2$ (47, 48; L = 44, 45), (L)$NiBr_2$ (49−51; L = 44−46), (L)$FeCl_2$ (52, 53; L = 44, 45), and (L)$CoCl_2$ (54, 55; L = 44, 45). These metal complexes of the bidentate ligands were prepared using methods similar to those described above. **47**: 80% yield, yellow powder, $\nu_{P=N}$ 1286 cm^{-1}. ^{31}P NMR (CD_2Cl_2, δ): 36.5 (s). ^{1}H NMR (CD_2Cl_2, δ): 8.45 (d, 1H, py), 7.25 (d, $J_{H-H} = 1$ Hz, 1H, py), 7.09−7.06 (m, 1H, py), 6.98 (t, $J_{H-H} = 3$ Hz, 1 H, py), 4.08 (s, 2H, CH_2). ^{13}C{H} NMR (CD_2Cl_2, δ): 156.8, 149.40, 135.9, 123.7, 128.0 (d, $J_{C-P} = 150$ Hz) 121.9, 122.0, 25.0. Anal. Calcd for $C_{24}H_{22}N_2PPdCl_2$: C, 52.80; H, 3.85; N, 5.13. Found: C, 51.82; H, 4.04; N, 5.42. **48**: 78% yield, yellow powder, $\nu_{P=N}$ 1279 cm^{-1}, ^{31}P NMR (CD_2Cl_2, δ): 37.0 (s). ^{1}H NMR (CD_2Cl_2, δ): 8.65 (d, $J_{H-H} = 3$ Hz, 2H, Ar), 8.57 (d, $J_{H-H} = 45$ Hz, 2H, Ar), 7.85−7.80 (m, 11H, Ar), 7.47 (d, $J_{H-H} = 2$ Hz, 1H, py), 7.25−7.09 (m, 1H, py), 7.08 (t, $J_{H-H} = 6$ Hz, 1H, py), 5.10 (s, 2H, CH_2), 2.54 (s, 3H, Me). ^{13}C{^{1}H} NMR (CD_2Cl_2, δ): 158.2, 136.1, 128.0 (d, $J_{C-P} = 120$ Hz), 120.0, 122.0, 26.0, 16.0. Anal. Calcd for $C_{25}H_{22}N_2PPdCl_2$: C, 51.40; H, 4.31; N, 8.00. Found: C, 50.78; H, 4.17; N, 8.42. **49**: 55% yield, purple powder, $\nu_{P=N}$ 1280 cm^{-1}, $\mu_{eff} = 2.35\ \mu_B$. ^{31}P{^{1}H} NMR (CD_2Cl_2): δ 41.3 (s). Anal. Calcd for $C_{24}H_{22}N_2PNiBr_2$: C, 50.13; H, 3.40; N, 4.77. Found: C, 50.40; H, 3.98; N, 5.14. **50**: 60% yield, purple powder. $\nu_{P=N}$ 1278 cm^{-1}, $\mu_{eff} = 2.98\ \mu_B$. ^{31}P{^{1}H} NMR (CD_2Cl_2, δ): 40.1 (s). Anal. Calcd for $C_{24}H_{22}N_2PNiBr_2$: C, 50.35; H,3.57; N, 4.78. Found: C, 50.12; H, 4.10; N, 5.01. **51**: 70% yield, purple powder, $\nu_{P=N}$ 1270 cm^{-1}, $\mu_{eff} = 3.02\ \mu_B$. ^{31}P{^{1}H} NMR (δ): 40.3 (s). Anal. Calcd for $C_{25}H_{23}N_2PNiBr_2$: C, 54.33; H, 3.77; N, 4.22. Found: C, 54.04; H, 4.17; N, 5.01. **52**: 60% yield. green powder, $\nu_{P=N}$ 1231 cm^{-1}, $\mu_{eff} = 4.98\ \mu_B$. Anal. Calcd for $C_{25}H_{23}N_2PFeCl_2$: C, 56.49; H, 4.47; N, 6.62. Found: C, 56.61; H, 4.99; N, 6.71. **53**: 65% yield, green powder, $\nu_{P=N}$ 1225 cm^{-1}, $\mu_{eff} = 5.11\ \mu_B$. Anal. Calcd for $C_{25}H_{22}N_2PFeCl_2$: C, 56.49; H, 4.47; N, 6.62. Found: C, 56.11; H, 4.17; N, 6.70. **54**: 70% yield, blue powder, $\nu_{P=N}$ 1260 cm^{-1}, $\mu_{eff} = 4.08\ \mu_B$. Anal. Calcd for $C_{24}H_{22}N_2PCoCl_2$: C. 57.85; H. 4.21; N. 5.62. Found: C. 57.64; H. 4.24; N. 5.70. **55**: 75% yield, blue powder, $\nu_{P=N}$ 1252 cm^{-1}, $\mu_{eff} = 5.23\ \mu_B$. Anal. Calcd for $C_{25}H_{22}N_2PCoCl_2$: C, 58.39; H, 4.71; N, 5.71. Found: C, 58.61; H, 4.82; N, 6.19.

Synthesis of 1-Me-2-(PPh_2)$C_3H_2N_2$ (58), 1-Me-2-(PPh_2)4,5-$Ph_2C_3N_2$ (59), 1-Me-2-(PPh_2)$C_7H_6N_2$ (60). Compounds **58**−**60** were prepared by similar methods; thus, only one representative procedure is described. To a cooled (−78 °C) THF (50 mL) solution of 1-Me-$C_3H_3N_2$ (5.0 g, 60.9 mmol) was added *n*-BuLi (28 mL, 2.5 M in hexanes, 70 mmol) dropwise. The solution was stirred for 1 h, and Ph_2PCl (12.0 mL, 67.1 mmol) was added in a dropwise fashion. The solution was gradually warmed to 25 °C and stirred overnight. The solvent was removed in vacuo, and Et_2O (75 mL) and H_2O (50 mL) were added. The organic layer was collected, and the aqueous layer was washed with ether (30 mL). The ether layer was dried over $MgSO_4$ and filtered, and the solvent was removed to give a white solid. The product was recrystallized with CH_2Cl_2/hexane to give a microcrystalline solid (90% yield). **58**: ^{31}P{^{1}H} NMR (δ): −30.0 (s). ^{1}H NMR (δ): 3.75 (s, 3H, −NMe), 7.05 (m, 1H, imid), 7.27 (d, 1 Hz, 1H, imid), 7.27−7.37 (m, 6H, *m*-PPh_2, *p*-PPh_2), 7.43−7.49 (m, 4H, *o*-PPh_2). ^{13}C{^{1}H} NMR (δ): 34.2 (d, $J_{C-P} = 14$ Hz), 123.8, 128.8 (d, $J_{C-P} = 8$ Hz), 129.3, 131.1, 134.1 (d, $J_{C-P} = 20$ Hz), 135.0 (d, $J_{C-P} = 4$ Hz), 146.0. **59**: 85% yield, white microcrystalline solid. ^{31}P{^{1}H} NMR (δ): −29.5 (s). ^{1}H NMR (δ): 3.55 (s, 3H, Me), 7.13 (m, 1H, imid), 7.19 (m, 2H, Ar H), 7.35−7.40 (m, 8H, *m*-PPh_2, *p*-PPh_2, Ar H), 7.45−7.47 (m, 3H, Ar H, imid), 7.51 (m, 2H, Ar H), 7.67−7.70 (m, 4H, *o*-PPh_2). ^{13}C{^{1}H} NMR (δ): 32.5 (d, $J_{C-P} = 15$ Hz), 126.2, 126.7, 128.0, 128.4 (d, $J_{C-P} = 8$ Hz), 128.6, 128.9, 129.0, 130.8, 131.3, 132.1, 134.0 (d, $J_{C-P} = 20$ Hz), 134.9, 135.5 (d, $J_{C-P} = 5$ Hz), 139.8, 145.0. **60**: 86% yield, white powder. ^{31}P{^{1}H} NMR (δ): −24.9 (s). ^{1}H NMR (δ): 3.83 (s, 3H, Me), 7.27 (m, 2H, benzimid), 7.32 (m, 1H, benzimid), 7.36−7.38 (m, 7H, *m*-PPh_2, *p*-PPh_2, benzimid), 7.51−7.54 (m, 4H, *o*-PPh_2), 7.83 (d, 1H, benzimid). ^{13}C{^{1}H} NMR (δ): 31.3 (d, $J_{C-P} = 14$ Hz), 109.4, 120.7, 122.2, 123.2, 129.0 (d, $J_{C-P} = 7.8$ Hz), 129.7, 133.9 (d, $J_{C-P} = 5$ Hz), 134.3 (d, $J_{C-P} = 20$ Hz), 137.2, 144.4 (d, $J_{C-P} = 7$ Hz), 154.3 (d, $^{2}J_{C-P} = 3$ Hz).

Synthesis of 1-Me-2-(2,6-$Me_2C_6H_3NPPh_2$)$C_3H_2N_2$ (61), 1-Me-2-(2,6-*i*-$Pr_2C_6H_3NPPh_2$)$C_3H_2N_2$ (62), 1-Me-2-(2,6-Me_2-

$C_6H_3NPPh_2$)-4,5-$Ph_2C_3N_2$ (63), 1-Me-2-(2,6-*i*-$Pr_2C_6H_3NPPh_2$)-4,5-$Ph_2C_3N_2$ (64), 1-Me-2-(2,6-$Me_2C_6H_3NPPh_2$)$C_7H_6N_2$ (65), 1-Me-2-(2,6-*i*-$Pr_2C_6H_3NPPh_2$)$C_7H_6N_2$ (66), 1-Me-2-(2,6-*i*-$Pr_2C_6H_3NPPh_2$)-4-*t*-BuC_3HN_2 (67). Compounds **61**−**67** were prepared by similar methods; thus, only one representative procedure is described. To a THF solution (50 mL) of **58** (1.50 g, 5.6 mmol) was added 2,6-$Me_2C_6H_3N_3$ (1.7 g, 10.2 mmol). The solution was heated at 60 °C overnight, and the solvent was subsequently removed to give a brown oil. Petroleum ether was added and the mixture was stirred at −30°C overnight. Filtration gave 2.0 g (93%) of a cream-colored solid, $\nu_{P=N}$ 1352 cm^{-1}. **61**: $^{31}P\{^1H\}$ NMR (δ): −16.0 (s).^{1}H NMR (δ): 1.96 (s, 6H, Me), 3.68 (s, 3H, NMe), 6.67 (dt, J_{H-H} = 8, 2 Hz, 1H, NAr H), 6.90 (d, 7 Hz, 2H, NAr H), 7.05 (m, 1H, imid), 7.23 (m, 1H, imid), 7.41−7.47 (m, 4H, *m*-PPh_2), 7.53 (dt, J_{H-H} = 6, 2 Hz, 2H, *p*-PPh_2), 7.69−7.77 (m, 4H, *o*-PPh_2). $^{13}C\{^1H\}$ NMR (δ): 18.2, 34.9, 119.6, 125.3, 127.5 (d, J_{C-P} = 12 Hz), 127.9, 128.7 (d, J_{C-P} = 13 Hz), 130.0 (d, J_{C-P} = 15 Hz), 131.9, 132.2 (d, J_{C-P} = 10 Hz), 132.7, 143.0 (J_{C-P} = 128 Hz), 145.8. **62**: 95% yield, cream-colored solid, $\nu_{P=N}$ 1358 cm^{-1}. $^{31}P\{^1H\}$ NMR (δ): −16.3 (s).^{1}H NMR (δ): 0.88 (d, 7 Hz, 12H, $CHMe_2$), 3.22 (sept, 7 Hz, 2H, −$CHMe_2$), 3.67 (s, 3H, Me), 6.85 (m, 1H, NAr H), 6.96 (m, 2H, NAr H), 7.04 (s, 1H, imid), 7.21 (s, 1H, imid), 7.42−7.46 (m, 4H, *m*-PPh_2), 7.52 (m, 2H, *p*-PPh_2), 7.66−7.70 (m, 4H, *o*-PPh_2). $^{13}C\{^1H\}$ NMR (δ): 23.0, 27.5, 34.9, 119.0, 124.9, 127.5 (d, J_{C-P} = 12 Hz), 127.9, 128.9 (d, J_{C-P} = 13 Hz), 130.9 (d, J_{C-P} = 16 Hz), 131.0, 132.0 (d, J_{C-P} = 10 Hz), 132.0, 144.0 (J_{C-P} = 129 Hz), 146.2. **63**: 92% yield, slightly yellow solid, $\nu_{P=N}$ 1361 cm^{-1}. $^{31}P\{^1H\}$ NMR (δ): −16.6 (s). ^{1}H NMR (δ): 2.03 (s, 6H, Me), 3.46 (s, 3H, NMe), 6.92 (m, 1H, NAr H), 6.93 (d, 7 Hz, 2H, NAr H), 7.15−7.18 (m, 3H, Ar H), 7.31−7.34 (m, 2H, Ar H), 7.46−7.55 (m, 11H, *m*-PPh_2, *p*-PPh_2, Ar H), 7.89−7.95 (m, 4H, *o*-PPh_2). $^{13}C\{^1H\}$ NMR (partial, δ): 20.2, 33.0, 119.1, 126.7, 127.9, 128.2 (d, $^2J_{C-P}$ = 13 Hz), 128.5, 129.1, 129.2, 130.3, 130.8, 131.7, 132.4 (d, J_{C-P} = 10 Hz), 132.6, 134.3, 138.7 (d, J_{C-P} = 14 Hz), 142.5 (d, J_{C-P} = 128 Hz), 146.5. **64**: 91% yield, cream-colored solid, $\nu_{P=N}$ 1372 cm^{-1}. $^{31}P\{^1H\}$ NMR (δ): −16.3 (s).^{1}H NMR (δ): 0.94 (d, 6.9 Hz, 12H, $CHMe_2$), 3.32 (sept, 7 Hz, 2H, $CHMe_2$), 3.44 (s, 3H, Me), 6.82 (dt, 7 Hz, 2 Hz, 1H, NAr H), 6.97 (m, 2H, NAr H), 7.13−7.27 (m, 3H, Ar H), 7.30−7.33 (m, 2H, Ar H), 7.42−7.58 (m, 11H, *m*-PPh_2, *p*-PPh_2, Ar H), 7.82−7.90 (m, 4H, *o*-PPh_2). $^{13}C\{^1H\}$ NMR (partial, δ): 23.7, 28.5, 32.8, 119.5, 122.7, 126.5, 126.8, 128.2 (d, J_{C-P} = 11.2 Hz), 128.4, 130.4 (d, J_{C-P} = 9 Hz), 130.6, 131.5, 132.0, 132.4 (d, J_{C-P} = 10 Hz), 133.1, 134.4, 138.7 (d, J_{C-P} = 14 Hz), 141.7, 142.7 (d, J_{C-P} = 8 Hz), 142.9 (d, J_{CP} 115 Hz), 143.3 (d, J_{C-P} = 13 Hz). **65**: 88% yield, beige solid, $\nu_{P=N}$ 1362 cm^{-1}. $^{31}P\{^1H\}$ NMR (d_8-THF, δ): −19.0 (s) ^{1}H NMR (δ): 1.95 (s, 6H, Me), 3.83 (s, 3H, NMe), 6.49 (dt, 7.5, 1.5 Hz, 1H, NAr H), 6.77 (d, 8 Hz, 2H, NAr H), 7.24−7.32 (m, 2H, benzimid), 7.41−7.52 (m, 7H, *m*-PPh_2, *p*-PPh_2, benzimid), 7.32 (d, 8 Hz, 1H, benzimid), 7.86−7.93 (m, 4H, *o*-PPh_2). $^{13}C\{^1H\}$ NMR (δ): 21.1, 25.8, 32.1, 111.1, 119.6, 122.0, 123.5, 125.1, 128.7, 129.3 (d, J_{C-P} = 13 Hz), 132.5, 132.6, 133.2 (d, J_{C-P} = 10 Hz), 134.2, 138.1 (d, J_{C-P} = 3 Hz), 144.2 (d, J_{C-P} = 16 Hz), 147.5, 150.5 (d, J_{C-P} = 122 Hz). **66**: 92% yield, cream-colored solid, $\nu_{P=N}$ 1370 cm^{-1}. $^{31}P\{^1H\}$ NMR (δ): −15.5 (s). ^{1}H NMR (δ): 0.83 (d, 12 H, 7 Hz, $CHMe_2$), 3.23 (sept, 2H, 7 Hz, $CHMe_2$), 3.84 (s, 3H, NMe), 6.80−6.86 (m, 1H, NAr H), 6.95 (d, 2H, NAr H), 7.25−7.35 (m, 1H, benzimid), 7.40 (m, 2H, benzimid), 7.44−7.50 (m, 4H, *m*-PPh_2), 7.53−7.58 (m, 2H, *p*-PPh_2), 7.73−7.80 (m, 4H, *o*-PPh_2), 7.86 (m, 1H, benzimid). $^{13}C\{^1H\}$ NMR (δ): 23.6, 28.7, 31.6, 109.6, 119.8, 121.6, 122.7, 124.4, 128.6 (d, J_{C-P} = 12.9 Hz), 130.6 (d, J_{C-P} = 112 Hz), 132.3 (d, J_{C-P} = 10 Hz), 133.1, 133.9, 137.0, 142.6 (d, J_{C-P} = 7 Hz), 142.8, 143.4 (d, J_{C-P} = 18 Hz), 150.7 (d, J_{C-P} = 121 Hz). **67**: 90% yield, yellow solid, $\nu_{P=N}$ 1377 cm^{-1}. $^{31}P\{^1H\}$ NMR (δ): −18.8 (s). ^{1}H NMR (δ): 0.85 (d, 12H, 7 Hz, $CHMe_2$), 1.21 (s, 9H, Me), 3.25 (sept, 2H, $CHMe_2$), 3.36 (s, 3H, NMe), 6.65 (s, 1H, imid), 6.80 (m, 1H, NAr H), 6.92 (m, 2H, NAr H), 7.37−7.40 (m, 4H, *m*-PPh_2), 7.44 (m, 2H, *p*-PPh_2), 7.76−7.80 (m, 4H, *o*-PPh_2). $^{13}C\{H\}$ NMR (δ): 22.6, 28.7, 30.2, 31.9, 34.1, 118.7, 119.1, 122.6, 128.1 (d, J_{C-P} = 13 Hz), 131.1, 132.3 (d, J_{C-P} = 10 Hz), 132.5 (d, J_{C-P} = 113 Hz) 141.5 (d, J_{C-P} = 131 Hz), 142.6 (d, J_{C-P} = 8 Hz), 143.6, 152.9 (d, J_{C-P} = 14 Hz).

Synthesis of (1-Me-2-(2,6-*i*-$Pr_2C_6H_3NPPh_2$)$C_3H_2N_2$)-$PdCl_2$·MeCN (68). To a stirred solution of $(PhCN)_2PdCl_2$ (44 mg, 0.11 mmol) in toluene was added a toluene solution (5 mL) of **62 (**50 mg, 0.11 mmol). The red solution was stirred for 2 h, and an orange precipitate gradually formed. After 2 h, the solution was cooled to −30 °C and filtered, and the solid was washed with cold toluene several times. The orange solid was recrystallized by dissolving in MeCN and cooling to −30 °C to give orange crystals. $^{31}P\{^1H\}$ NMR (d_6-DMSO, δ): 28.2 (s). ^{1}H NMR (d_6-DMSO, δ): 0.27 (d, J_{H-H} = 7 Hz, 6H, $CHMe_2$), 1.32 (d, J_{H-H} = 7 Hz, 6H, $CHMe_2$), 3.30 (s, 3H, NMe), 3.32 (sept, 7 Hz, 2H, $CHMe_2$), 6.76 (d, J_{H-H} = 8 Hz, 2H, NAr H), 6.96 (dt, J_{H-H} = 8 Hz, 2 Hz, 1H, NAr H), 7.65−7.72 (m, 8H, *m*-PPh_2, *p*-PPh_2, imid), 7.77−7.82 (m, 4H, *o*-PPh_2). $^{13}C\{^1H\}$ NMR (d_6-DMSO, δ): 22.5, 25.1, 28.3, 35.8, 122.0, 123.1, 123.3, 125.3, 128.6, 129.9 (d, J_{C-P} = 15 Hz), 132.5 (d, J_{C-P} = 10 Hz), 134.5, 137.2, 140.0 (d, J_{C-P} = 165 Hz), 147.2 (d, J_{C-P} = 5 Hz). Anal. Calcd for $C_{30}H_{35}Cl_2N_4PPd$ (659.93): C, 54.60; H, 5.35; N, 8.49. Found: C, 54.13; H, 5.29; N, 8.39.

Synthesis of (L)$NiBr_2$ (69−75; L = 61−67). Compounds **69**−**75** were prepared by similar methods; thus, only one representative procedure is described. To a slight excess of **61** (1.05 equiv, 150 mg, 0.39 mmol) and $NiBr_2$(DME) adduct (114 mg, 0.37 mmol) was added 10 mL of CH_2Cl_2. The blue suspension was stirred overnight and concentrated in vacuo. Et_2O (10 mL) was added, and the mixture was filtered to give a light blue powder. **69**: 95% yield, purple powder, $\nu_{P=N}$ 1225 cm^{-1}, μ_{eff} = 3.01 μ_B. Anal. Calcd for $C_{24}H_{24}Br_2N_3NiP$ (603.94): C, 47.73; H, 4.01; N, 6.96. Found: C, 47.68; H, 4.00; N, 6.82. **70**·CH_2Cl_2: 90% yield, blue-green powder, $\nu_{P=N}$ 1214 cm^{-1}, μ_{eff} = 2.94 μ_B. Anal. Calcd for $C_{29}H_{34}Br_2Cl_2N_3NiP$ (744.98): C, 46.75; H, 4.60; N, 5.64. Found: C, 46.47; H, 4.44; N, 6.01. **71**: 90% yield, purple powder, $\nu_{P=N}$ 1217 cm^{-1}, μ_{eff} = 2.99 μ_B. Anal. Calcd for $C_{36}H_{32}Br_2N_3NiP$ (756.13): C, 57.18; H, 4.27; N, 5.56. Found: C, 56.83; H, 4.47; N, 5.33. **72**: 87% yield, blue-green powder, $\nu_{P=N}$ 1196 cm^{-1}, μ_{eff} = 3.15 μ_B. Anal. Calcd for $C_{40}H_{40}Br_2N_3NiP$ (812.24): C, 59.15; H, 4.96; N, 5.17. Found: C, 59.41; H, 5.13; N, 5.01. **73**·CH_2Cl_2: 86% yield, purple powder, $\nu_{P=N}$ 1219 cm^{-1}, μ_{eff} = 3.41 μ_B. Anal. Calcd for $C_{29}H_{28}Br_2Cl_2N_3NiP$ (738.93): C, 47.14; H, 3.82; N, 5.69. Found: C, 47.42; H, 3.66; N, 5.84. **74**: 87% yield, blue-green powder, $\nu_{P=N}$ 1243 cm^{-1}, μ_{eff} = 3.24 μ_B. Anal. Calcd for $C_{32}H_{32}Br_2N_3NiP$ (708.09): C, 54.28; H, 4.56; N, 5.93. Found: C, 54.57; H, 4.10; N, 5.81. **75**: 91% yield, blue-green powder, $\nu_{P=N}$ 1244 cm^{-1}, μ_{eff} = 3.07 μ_B. Anal. Calcd for $C_{32}H_{40}Br_2N_3NiP$ (716.16): C, 53.67; H, 5.63; N, 5.87. Found: C, 53.14; H, 5.44; N, 5.83.

Synthesis of (L)$FeCl_2$ (76−82; L = 61−67). Compounds **76**−**82** were prepared by similar methods; thus, only one representative procedure is described. To a slight excess of **61** (150 mg, 0.39 mmol) and $FeCl_2$ (47 mg, 0.37 mmol) was added THF (10 mL). The orange suspension was stirred overnight and was then concentrated in vacuo. Et_2O (10 mL) was added, and the mixture was filtered to give an orange powder. **76**: 88% yield, orange solid, $\nu_{P=N}$ 1211 cm^{-1}, μ_{eff} = 4.98 μ_B. Anal. Calcd for $C_{24}H_{24}Cl_2N_3FeP$ (512.19): C, 56.28; H, 4.72; N, 8.20. Found: C, 55.97; H, 4.80; N, 7.86. **77**: 95% yield, yellow-orange solid, $\nu_{P=N}$ 1198 cm^{-1}, μ_{eff} = 5.10 μ_B. Anal. Calcd for $C_{28}H_{32}Cl_2N_3FeP$ (568.30): C, 59.18; H, 5.68; N, 7.39. Found: C, 58.89; H, 6.00; N, 7.43. **78**: 84% yield, yellow crystals, $\nu_{P=N}$ 1217 cm^{-1}, μ_{eff} = 5.01 m$_B$. Anal. Calcd for $C_{36}H_{32}Cl_2N_3FeP$ (664.38): C, 65.08; H, 4.85; N, 6.32. Found: C, 64.91; H, 4.52; N, 5.82. **79**·2CH_2Cl_2: 85% yield, yellow crystals, $\nu_{P=N}$ 1120 cm^{-1}, μ_{eff} = 4.99 μ_B. Anal. Calcd for $C_{42}H_{44}Cl_6FeN_3P$ (890.35): C, 56.66; H, 4.98; N, 4.72. Found: C, 56.55; H, 4.64; N, 4.93. **80**: 89% yield, orange solid, $\nu_{P=N}$ 1215 cm^{-1}, μ_{eff} = 5.24 μ_B. Anal. Calcd for $C_{28}H_{26}Cl_2N_3FeP$ (562.25): C, 59.81; H, 4.66; N, 7.47. Found: C, 59.65; H, 5.06; N, 7.77. **81**: 92% yield, yellow-orange solid,

$\nu_{P=N}$ 1191 cm^{-1}, μ_{eff} = 5.21 μ_B. Anal. Calcd for $C_{32}H_{34}Cl_2N_3FeP$ (618.36): C, 62.16; H, 5.54; N, 6.80. Found: C, 61.78; H, 5.85; N, 7.11. **82**: 80% yield, yellow crystals, $\nu_{P=N}$ 1193 cm^{-1}, μ_{eff} = 5.12 μ_B. Anal. Calcd for $C_{32}H_{40}Cl_2N_3FeP$ (624.40): C, 61.55; H, 6.46; N, 6.73. Found: C, 61.15; H, 6.38; N, 6.88.

Procedure for Ethylene Polymerization/Oligomerization. A 500 mL Parr stainless steel autoclave equipped with mechanical stirring and pressure gauge was heated (~110 °C) under vacuum for >2 h. The temperature of the autoclave was regulated by a thermal jacket. The autoclave was cooled to the desired temperature, and 500 equiv of MAO dissolved in toluene was added under N_2. The solution was stirred for an additional 1 h, and a toluene suspension of the catalyst was added. The vessel was then quickly pressurized with 300 psi of ethylene, and the reaction mixture was stirred for 30 min. The polymerization was stopped by venting the volatiles at 25 °C, followed by quenching of the reaction solution with acidified MeOH, and the solution filtered. The organic layer was separated, dried with Na_2SO_4, and filtered. The solvent was removed to give traces of a sticky, gummy polymer. The trace amounts of polymer were redissolved in hexane, the solution was filtered again to remove any residual catalyst, and the solvent was removed.

In the case of oligomerization, after reaction the autoclave was cooled to −78 °C, and the volatiles were slowly vented. EtOH (20 mL) and an internal standard were added (toluene (DEAC activation) or Et_2O (MAO activation)) to quench the reaction, and the mixture was slowly warmed to −30 °C over 10 min. The composition of the alkenes formed was determined by GC and NMR spectroscopy.

Computational Details. Optimized geometries of $[(L)NiMe]^+$ (L = diimine (NCCN), phosphinimine−imine (NPCN), and fluorinated phosphinimine−imine (NPF_2CN)) were obtained using the Gaussian 98[32] suite of programs. The hybrid DFT method B3LYP (Becke, 1998, #63; as implemented in G98) was employed in conjunction with the 6-31G(d) basis set for the ligand and the LANL2DZ basis set for nickel. This latter basis set uses the effective core potentials developed by Hay and Wadt.[33] NBO analysis was also performed on the optimized structure to determine the natural charge on the nickel atom. The optimized geometry of the Ni complex was used to determine the orbital energies of the ligand. After the Cartesian coordinates were determined for each optimized structure, the nickel and methyl species were removed. A single-point energy calculation was then performed on the resulting constrained ligand geometries using the Hartree−Fock (HF) method and the 6-31G(d) basis set to determine the lone pair orbital energy. Lone pair diagrams were generated using POV-ray.

X-ray Data Collection and Reduction. X-ray-quality crystals were obtained directly from the preparations as described above. The crystals were manipulated and mounted in capillaries in a glovebox, thus maintaining a dry, O_2-free environment for each crystal. Diffraction experiments were performed on a Siemens SMART System CCD diffractometer. The data were collected for a hemisphere of data in 1329 frames with 10 s exposure times. Crystal data are summarized in Table 2. The observed extinctions were consistent with the space groups in each case. A measure of decay was obtained by re-collecting the first 50 frames of each data set. The

Table 1. Compound Numbering: Ligands and Ni, Fe, and Co Complexes

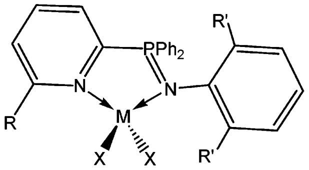

$(2,6\text{-}R_2C_6H_3N)2\text{-}(PPh_2)6\text{-}(R')C_5H_3N$				
R'	R	Ligand	(L)$NiBr_2$	(L)$FeCl_2$
Me	H	**10**	**21**	**31**
i-Pr	H	**11**	**22**	**32**
Me	Me	**12**	**23**	**33**
i-Pr	Me	**13**	**24**	**34**
Me	Bn	**14**	**25**	**35**
i-Pr	Bn	**15**	**26**	**36**
Me	$SiMe_3$	**16**	**27**	**37**
i-Pr	$SiMe_3$	**17**	**28**	**38**
Me	Ph	**18**	**29**	**39**
i-Pr	Ph	**19**	**30**	**40**

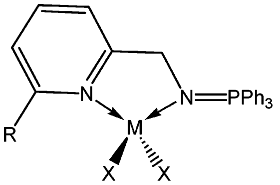

$(6\text{-}RC_5H_3N)CH_2NPPh_3$				
R	Ligand	(L)$NiBr_2$	(L)$FeCl_2$	(L)$CoCl_2$
H	**44**	**49**	**52**	**54**
Me	**45**	**50**	**53**	**55**
Ph	**46**	**51**		

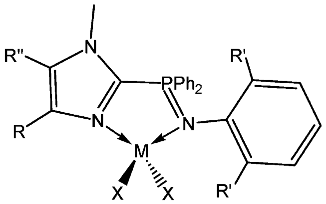

$(2,6\text{-}R_2C_6H_3N)2\text{-}(PPh_2)3\text{-}(Me)4\text{-}(R'')5\text{-}(R)C_3N_2$				
R'	R/R"	Ligand	(L)$NiBr_2$	(L)$FeCl_2$
Me	H	**61**	**69**	**76**
i-Pr	H	**62**	**70**	**77**
Me	Ph	**63**	**71**	**78**
i-Pr	Ph	**64**	**72**	**79**
Me	C_4H_4	**65**	**73**	**80**
i-Pr	C_4H_4	**66**	**74**	**81**
i-Pr	*t*-Bu/H	**67**	**75**	**82**

---

[32] Frisch, M. J.; Trucks, G. W.; Schlegel, H. B.; Scuseria, G. E.; Robb, M. A.; Cheeseman, J. R.; Zakrzewski, V. G.; Montgomery, J. A. J.; Stratmann, R. E.; Burant, J. C.; Dapprich, S.; Millam, J. M.; Daniels, A. D. K., K. N.; Strain, M. C.; Farkas, O.; Tomasi, J.; Barone, V.; Cossi, M.; Cammi, R.; Mennucci, B.; Pomelli, C.; Adamo, C.; Clifford, S.; Ochterski, J.; Petersson, G. A.; Ayala, P. Y.; Cui, Q.; Morokuma, K.; Salvador, P.; Dannenberg, J. J.; Malick, D. K.; Rabuck, A. D.; Raghavachari, K.; Foresman, J. B.; Cioslowski, J.; Ortiz, J. V.; Baboul, A. G.; Stefanov, B. B.; Liu, G.; Liashenko, A.; Piskorz, P.; Komaromi, I.; Gomperts, R.; Martin, R. L.; Fox, D. J.; Keith, T.; Al-Laham, M. A.; Peng, C. Y.; Nanayakkara, A.; Challacombe, M.; Gill, P. M. W.; Johnson, B.; Chen, W.; Wong, M. W.; Andres, J. L.; Gonzalez, C.; Head-Gordon, M.; Replogle, E. S.; Pople, J. A. Gaussian 98; Gaussian, Inc., Pittsburgh, PA, 2001.

[33] Hay, P. J.; Wadt, W. R. *J. Chem. Phys.* **1985**, *82*, 270−283.

Table 2. Crystallographic Parameters[a]

	2	**20**	**26**	**27**·CH_2Cl_2	**35**	**37**	**40**·H_2O
formula	$C_{18}H_{16}NP$	$C_{20}H_{23}Cl_2N_2PPdSi$	$C_{36}H_{37}Br_2N_2NiP$	$C_{29}H_{33}Br_2Cl_2N_2NiPSi$	$C_{32}H_{30}Cl_2FeN_2P$	$C_{28}H_{31}Cl_2FeN_2PSi$	$C_{35}H_{37}Cl_2FeN_2OP$
fw	277.29	527.76	747.18	758.06	600.30	581.36	659.39
a (Å)	11.076(7)	9.426(14)	20.150(14)	10.109(6)	16.655(9)	8.807(4)	9.019(5)
b (Å)	9.274(6)	15.17(2)	9.089(6)	20.839(14)	20.504(11)	9.436(5)	17.963(9)
c (Å)	15.069(10)	15.75(2)	18.691(12)	15.184(9)	9.028(5)	18.571(9)	21.636(11)
α (deg)		90.83(3)				101.385(8)	
β (deg)		91.56(3)	102.377(14)	92.665(13)		98.601(9)	99.174(10)
γ (deg)		90.18(3)				96.586(10)	
cryst syst	orthorhombic	triclinic	monoclinic	monoclinic	orthorhombic	triclinic	monoclinic
space group	$Pna2_1$	$P\bar{1}$	$P2_1/c$	$P2_1/n$	$Pna2_1$	$P\bar{1}$	$P2_1/c$
V (Å^3)	1547.9(16)	2252(6)	3344(4)	3195(4)	3083(3)	1479.3(13)	3460(3)
D_{calcd} (g cm^{-3})	1.190	1.556	1.484	1.576	1.293	1.305	1.266
Z	4	4	4	4	4	2	4
abs coeff, μ, mm^{-1}	0.167	1.193	3.045	3.385	0.737	0.804	0.665
no. of data collected	6176	9555	13 890	13 144	12 795	6296	14 566
no. of data with $F_o^2 > 3\sigma(F_o^2)$	2130	6435	4819	4564	4326	4183	4882
no. of variables	181	487	379	343	343	316	387
R (%)	0.0289	0.0262	0.0573	0.0790	0.0552	0.0339	0.0410
R_w (%)	0.0639	0.0667	0.1032	0.2018	0.1390	0.1102	0.1076
goodness of fit	0.702	1.066	0.811	1.023	0.975	0.995	0.711

	49	**50**	**51**·H_2O	**54**	**68**·MeCN	**79**·$2CH_2Cl_2$	**82**
formula	$C_{24}H_{21}Br_2N_2NiP$	$C_{25}H_{23}Br_2N_2NiP$	$C_{30}H_{29}Br_2N_2NiO_2P$	$C_{25}H_{23}Cl_2CoN_2P$	$C_{30}H_{32}Cl_2N_4PPd$	$C_{42}H_{44}Cl_6FeN_3P$	$C_{32}H_{40}Cl_2FeN_3P$
fw	586.93	600.95	699.04	512.26	656.87	890.32	624.39
a (Å)	9.272(6)	8.090(4)	12.238(7)	20.261(11)	10.333(8)	16.006(9)	12.376(6)
b (Å)	13.665(8)	19.942(10)	11.229(6)	15.214(8)	11.302(8)	18.784(11)	15.765(8)
c (Å)	19.814(12)	15.744(8)	22.877(13)	16.155(9)	13.339(10)	16.330(9)	17.919(8)
α (deg)					73.674(14)		
β (deg)	101.227(10)	96.610(9)	101.244(11)	99.234(10)	87.098(13)	113.890(11)	109.685(9)
γ (deg)					85.621(14)		
cryst syst	monoclinic	monoclinic	monoclinic	monoclinic	triclinic	monoclinic	monoclinic
space group	$P2_1/c$	$P2_1/c$	P2(1)	$C2/c$	$P\bar{1}$	$P2_1/n$	$P2_1/c$
V (Å^3)	2462(3)	2523(2)	3083(3)	4915(5)	1490.0(19)	4489(4)	3292(3)
D_{calcd} (g cm^{-3})	1.583	1.582	1.467	1.384	1.464	1.317	1.260
Z	4	4	4	8	2	4	4
abs coeff, μ, mm^{-1}	4.111	4.014	3.297	0.996	0.882	0.761	0.694
no. of data collected	10 362	10 676	13 500	10 443	6265	18 964	13 829
no. of data with $F_o^2 > 3\sigma(F_o^2)$	3505	3595	8248	3521	4278	6369	4674
no. of variables	271	280	673	280	343	478	352
R (%)	0.0286	0.0301	0.0612	0.0290	0.0431	0.0519	0.0311
R_w (%)	0.0807	0.0730	0.1486	0.0586	0.1046	0.1396	0.0841
goodness of fit	0.338	0.985	0.927	0.820	1.004	0.978	1.005

[a] All data were collected at 24 °C with Mo Kα radiation ($\lambda = 0.710\ 69$ Å), $R = \sum||F_o| - |F_c||/\sum|F_o|$, $R_w = [\sum[w(F_o^2 - F_c^2)^2]/\sum[w(F_o^2)^2]]^{0.5}$.

intensities of reflections within these frames showed no statistically significant change over the duration of the data collections. An empirical absorption correction based on redundant data was applied to each data set. Subsequent solution and refinement was performed using the SHELXTL solution package.

Structure Solution and Refinement. Non-hydrogen atomic scattering factors were taken from the literature tabulations.[34] The heavy-atom positions were determined using direct methods. The remaining non-hydrogen atoms were located from successive difference Fourier map calculations. The refinements were carried out by using full-matrix least-squares techniques on F, minimizing the function $w(F_o - F_c)^2$, where the weight w is defined as $4F_o^2/2\sigma(F_o^2)$ and F_o and F_c are the observed and calculated structure factor amplitudes. For noncentrosymmetric space groups, the correct enantiomorph was confirmed by data inversion and refinement. In the final cycles of each refinement, all non-hydrogen atoms were assigned anisotropic temperature factors. Carbon-bound hydrogen atom positions were calculated and allowed to ride on the carbon to which they are bonded, assuming a C−H bond length of 0.95 Å. Hydrogen atom temperature factors were fixed at 1.10 times the isotropic temperature factor of the carbon atom to which they are bonded. The hydrogen atom contributions were calculated but not refined. The final values of refinement parameters are given in Table 2. Positional parameters, hydrogen atom parameters, thermal parameters, and bond distances and angles have been deposited as Supporting Information.

Results and Discussion

Pyridine−Phosphinimine (Endocyclic P) Ligand Complexes. A series of 2-substituted diphenylphosphine pyridines were synthesized in reasonable yields by the reaction of $LiPPh_2$ with the appropriately substituted bromopyridine precursor (Scheme 1). The ^1H NMR spectra of **1**−**6** showed the expected resonances with ^{31}P resonances around −3.5 ppm. In the case of **4**, X-ray crystallography confirmed the formulation (Figure 1). As expected, the geometry at the phosphorus atom is pseudo-tetrahedral with angles about P(1) ranging from 100.64(17) to 102.41(16)°, comparable to those previously reported for **1**.[35]

Substituted phenyl azides were synthesized, employing a modification of the published method.[31] The

---

[34] Cromer, D. T.; Mann, J. B. *Acta Crystallogr., Sect. A* **1968**, *A24*, 321−324.

[35] Dunne, B. J.; Orpen, A. G. *Acta Crystallogr., Sect. C* **1991**, *C47*, 345−347.

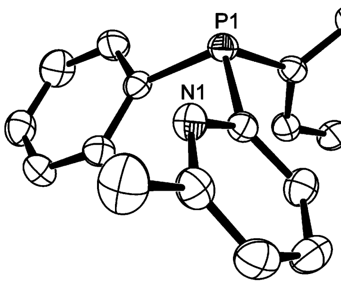

Figure 1. ORTEP drawing of **2**, with 30% thermal ellipsoids. H atoms have been omitted for clarity. Bond lengths (Å) and angles (deg): P(1)−C(1) = 1.846(2), P(1)−C(7) = 1.846(3), P(1)−C(13) = 1.850(3); C(1)−P(1)−C(7) = 102.29(12), C(1)−P(1)−C(13) = 100.90(12), C(7)−P(1)−C(13) = 100.94(12).

Scheme 1

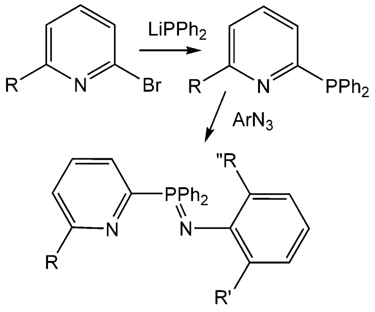

previously published syntheses[17,36] of 2,6-di-isopropylphenyl azide suffers from low yields and impurities. The method described herein involves the isolation of the air-stable diazonium tetrafluoroborate salt and subsequent nucleophilic reaction with azide to form **7** and **8** in yields greater than 85% yield, with only trace amounts of impurities. Oxidation of the phosphines **1**−**5** with **7**, **8**, or Me_3SiN_3 proceeded cleanly to give the series of phosphinimine derivatives **9**−**19** in excellent yields. These phosphinimine derivatives result in the observed downfield shift of the ^{31}P resonance to 5−10 ppm. The IR spectra of **9**−**19** were consistent with the presence of the P−N bonds with stretching frequencies ranging from 1329 to 1357 cm^{-1}, in agreement with previous results.[37−40] In an analogous method, attempts to oxidize the fluorinated phosphine 2-$P(C_6F_5)_2$6-PhC_5H_3N (**6**) were unsuccessful, despite the use of elevated temperatures. Similar difficulties with the oxidation of analogous pyrrolyl and indolyl phosphines have been previously reported.[41]

Reaction of the ligand **9** and $PdCl_2(PhCN)_2$ gives the square-planar, diamagnetic compound **20**, which can be identified by NMR spectroscopy. The ^1H NMR spectrum of complex **20** shows very little shift in the ligand resonances upon coordination to Pd; however, the ^{31}P NMR resonance displays the expected significant downfield shift of ca. 30 ppm. The formulation of **20** was also confirmed crystallographically. The geometry about Pd is pseudo square planar, with the pyridine−phosphinimine ligand coordinating in a bidentate fashion (Figure 2). The palladium−phosphinimine five-membered metallacycle is not planar, with a torsion angle formed by Pd(1)−N(2)−C(13)−P(1) of 4.3° and a mean deviation from the plane of 0.0847 Å. Such a distortion is not surprising, as Arques et al. have described this phenomenon for related complexes.[42] The Pd−Cl bond lengths (2.286(3), 2.280(2) Å), while chemically distinct, are very similar, suggesting that the trans influences of the two differing N-atom donors are similar. The Pd−phosphinimine N atom ($Pd-N_{Phos}$) bond is similar to those previously described for related Pd complexes of P,N-chelated phosphinimine ligands.[42,43] Although the P−N bond is slightly longer in **20** (1.578(3) Å) than that reported for the free ligand $CH_2(Ph_2P\text{-}NC_6H_4Me\text{-}4)_2$[14] (1.568(2) Å), this distance is typical of a highly polarized P−N bond.

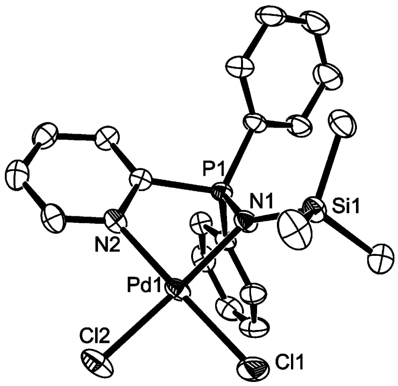

Figure 2. ORTEP drawing of one of the two molecules in the asymmetric unit of **20**, with 30% thermal ellipsoids. Hydrogen atoms have been omitted for clarity. Bond lengths (Å) and angles (deg): Pd(1)−N(2) = 2.056(4), Pd(1)−N(1) = 2.062(3), Pd(1)−Cl(2) = 2.280(2), Pd(1)−Cl(1) = 2.286(3), Pd(1)−P(1) = 2.873(3), P(1)−N(1) = 1.578(3), N(1)−Si(1) = 1.752(3); N(2)−Pd(1)−N(1) = 85.17(12), N(2)−Pd(1)−Cl(2) = 93.15(10), N(1)−Pd(1)−Cl(2) = 176.24(8), N(2)−Pd(1)−Cl(1) = 172.36(8), N(1)−Pd(1)−Cl(1) = 92.64(11), Cl(2)−Pd(1)−Cl(1) = 89.45(9), N(2)−Pd(1)−P(1) = 61.81(12), N(1)−Pd(1)−P(1) = 32.30(8), Cl(2)−Pd(1)−P(1) = 148.47(4), Cl(1)−Pd(1)−P(1) = 113.15(11), P(1)−N(1)−Si(1) = 134.77(16), P(1)−N(1)−Pd(1) = 103.42(14), Si1 N(1)−Pd(1) = 121.81(15).

Similarly, the Ni(II) and Fe(II) complexes **21**−**30** and **31**−**40,** respectively, were synthesized from the reaction between the ligands **10**−**19** and the corresponding metal halides (Table 1). The formulations of these metal complexes were supported by IR spectroscopy, magnetic susceptibility, elemental analysis, and X-ray crystallography. IR spectroscopy of these complexes showed $\nu_{P=N}$ bands between 1190 and 1250 cm^{-1}, which were about 100 cm^{-1} lower than those for the free ligands.[4,5] This suggests a slightly less polar P−N double-bond character upon ligand coordination, consistent with

---

(36) Smolinsky, G. *J. Org. Chem.* **1961**, *26*, 4108−4110.

(37) King, R. B.; Cloyd, J. C., Jr. *Inorg. Chem.* **1975**, *14*, 1550−1554.

(38) Hietkamp, S.; Stufkens, D. J.; Vrieze, K. *J. Organomet. Chem.* **1979**, *169*, 107−113.

(39) MacLeod, I.; Manojlovic-Muir, L.; Millington, D.; Muir, K. W.; Sharp, D. W. A.; Walker, R. *J. Organomet. Chem.* **1975**, *97*, C7−C10.

(40) Appleton, T. G.; Bennett, M. A. *Inorg. Chem.* **1978**, *17*, 738−747.

(41) Ali, R.; Dillon, K. B. *J. Chem. Soc., Dalton Trans.* **1990**, 2593−2596.

(42) Arques, A.; Molina, P.; Aunon, D.; Vilaplana, M. J.; Velasco, M. D.; Martinez, F.; Bautista, D.; Lahoz, F. J. *J. Organomet. Chem.* **2000**, *598*, 329−338.

(43) Liu, C.-Y.; Chen, D.-Y.; Cheng, M.-C.; Peng, S.-M.; Liu, S.-T. *Organometallics* **1995**, *14*, 1983−1991.

(44) Moore, S. S.; Whitesides, G. M. *J. Org. Chem.* **1982**, *47*, 1489−1493.

(45) Abdul Jalil, M.; Yamada, T.; Fujinami, S.; Honjo, T.; Nishikawa, H. *Polyhedron* **2001**, *20*, 627−633.

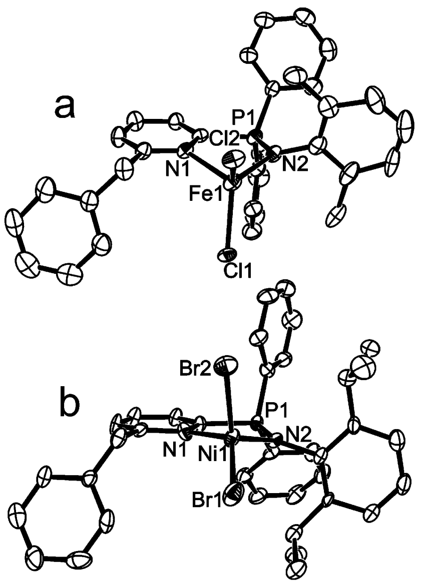

Figure 3. ORTEP drawings of (a) **35** and (b) **26**, with 30% thermal ellipsoids. Hydrogen atoms have been omitted for clarity. Bond lengths (Å) and angles (deg) for **35**: Fe(1)−N(2) = 2.053(6), Fe(1)−N(1) = 2.184(5), Fe(1)−Cl(2) = 2.317(2), Fe(1)−Cl(1) = 2.325(2), P(1)−N(2) = 1.608(6); N(2)−Fe(1)−N(1) = 84.3(2), N(2)−Fe(1)−Cl(2) = 116.93(17), N(1)−Fe(1)−Cl(2) = 113.84(16), N(2)−Fe(1)−Cl(1) = 112.01(17), N(1)−Fe(1)−Cl(1) = 108.07(17), Cl(2)−Fe(1)−Cl(1) = 116.97(8), P(1)−N(2)−Fe(1) = 116.8(3), Bond lengths (Å) and angles (deg) for **26**: Ni(1)−N(2) = 1.999(7), Ni(1)−N(1) = 2.062(7), Ni(1)−Br(1) = 2.355(2), Ni(1)−Br(2) = 2.4006(19), P(1)−N(2) = 1.613(7); N(2)−Ni(1)−N(1) = 87.6(3), N(2)−Ni(1)−Br(1) = 120.4(2), N(1)−Ni(1)−Br(1) = 126.1(2), N(2)−Ni(1)−Br(2) = 116.5(2), N(1)−Ni(1)−Br(2) = 102.0(2), Br(1)−Ni(1)−Br(2) = 103.51(7), P(1)−N(2)−Ni(1) = 114.2(4).

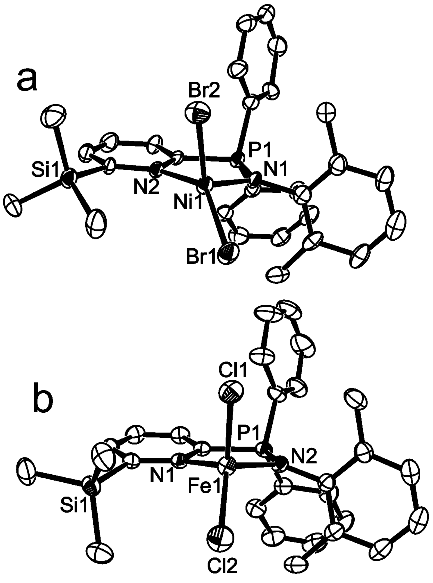

Figure 4. ORTEP drawings of (a) **27** and (b) **37**, with 30% thermal ellipsoids. Hydrogen atoms have been omitted for clarity. Bond lengths (Å) and angles (deg) for **27**: Ni(1)−N(1) = 1.996(8), Ni(1)−N(2) = 2.092(8), Ni(1)−Br(1) = 2.379(2), Ni(1)−Br(2) = 2.395(2), P(1)−N(1) = 1.586(9); N(1)−Ni(1)−N(2) = 88.4(3), N(1)−Ni(1)−Br(1) = 106.0(2), N(2)−Ni(1)−Br(1) = 139.4(2), N(1)−Ni(1)−Br(2) = 113.7(2), N(2)−Ni(1)−Br(2) = 100.6(2), Br(1)−Ni(1)−Br(2) = 107.36(7), P(1)−N(1)−Ni(1) = 115.2(4). Bond lengths (Å) and angles (deg) for **37**: Fe(1)−N(2) = 2.048(2), Fe(1)−N(1) = 2.192(2), Fe(1)−Cl(2) = 2.2451(11), Fe(1)−Cl(1) = 2.2737(10), P(1)−N(2) = 1.600(2); N(2)−Fe(1)−N(1) = 85.46(8), N(2)−Fe(1)−Cl(2) = 114.96(7), N(1)−Fe(1)−Cl(2) = 113.99(6), N(2)−Fe(1)−Cl(1) = 106.80(6), N(1)−Fe(1)−Cl(1) = 111.61(6), Cl(2)−Fe(1)−Cl(1) = 119.03(5), P(1)−N(2)−Fe(1) = 116.87(11).

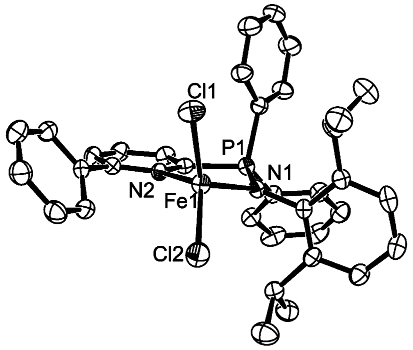

Figure 5. ORTEP drawing of **40**, with 30% thermal ellipsoids. Hydrogen atoms have been omitted for clarity. Bond lengths (Å) and angles (deg): Fe(1)−N(1) = 2.067(3), Fe(1)−N(2) = 2.229(3), Fe(1)−Cl(2) = 2.2668(16), Fe(1)−Cl(1) = 2.2754(15), P(1)−N(1) = 1.602(3); N(1)−Fe(1)−N(2) = 82.93(13), N(1)−Fe(1)−Cl(2) = 110.22(10), N(2)−Fe(1)−Cl(2) = 125.71(10), N(1)−Fe(1)−Cl(1) = 119.09(10), N(2)−Fe(1)−Cl(1) = 104.78(10), Cl(2)−Fe(1)−Cl(1) = 112.02(6), P(1)−N(1)−Fe(1) = 116.07(18).

X-ray data (vide infra). Magnetic susceptibility measurements showed average typical values of 5.13 μ_B for Fe(II) complexes and 3.04 μ_B for Ni(II) complexes.

In addition to these data, X-ray structure determinations were obtained for **26**, **27**, **35**, **37**, and **40** (Figures 3−5). The geometries about the metal atoms in these species are pseudo-tetrahedral, with two halides and a bidentate pyridine−phosphinimine ligand completing the coordination sphere. In all of these compounds the aryl ring on the N, as a result of the 2,6-substitution, is oriented approximately orthogonal to the ligand plane, a feature that has been shown to favor catalytic activity in related systems. The Ni−Br distances in **26** and **27** were similar, falling in the range from 2.355(2) to 2.4006(19) Å. In contrast, the Fe−Cl distances in **35** were 2.317(2) and 2.325(2) Å, which were significantly shorter than those found in **37** (2.2451(11), 2.2737(10) Å) and **40** (2.2668(16), 2.2754(15) Å). This difference may be attributed to the increasing steric effects of the $SiMe_3$ substituent on the pyridine ring. Of the two types of M−N bonds, the M−pyridine bond was consistently longer than the corresponding M−phosphinimine bond. For example, in **35** the Fe−N_{py} bond was found to be 2.184(5) Å, whereas the Fe−N_{Phos} bond was found to be 2.053(6) Å. Such differences are also amplified by sterically demanding substitution on the pyridine ring. In **37**, the difference between Fe−N_{py} and Fe−N_{Phos} increases to 0.144 Å in Fe−N_{Phos}, whereas in **40** this difference is further increased to 0.162 Å. Similarly, the Ni−N_{py} and Ni−N_{Phos} distances in **26** were found to be 2.062(7) and 1.999(7) Å, respectively; whereas in **27**, the corresponding distances are 2.092(8) and 1.996(8) Å. This again reflects the increased steric demand of $SiMe_3$ versus a benzyl group. The P−N bond lengths in these compounds varied between 1.586(9) and 1.613(7) Å, which is typical of coordinated phosphinimine ligands.[46] For example, Elsevier et al. reported similar P−N

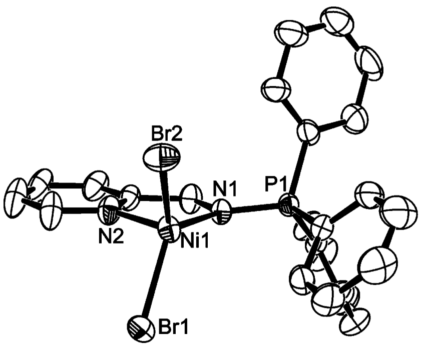

Figure 6. ORTEP drawing of **49**, with 30% thermal ellipsoids. Hydrogen atoms have been omitted for clarity. Bond lengths (Å) and angles (deg): Ni(1)−N(2) = 1.976(5), Ni(1)−N(1) = 1.977(4), Ni(1)−Br(2) = 2.3611(16), Ni(1)−Br(1) = 2.3832(13), P(1)−N(1) = 1.615(5); N(2)−Ni(1)−N(1) = 83.69(19), N(2)−Ni(1)−Br(2) = 108.59(14), N(1)−Ni(1)−Br(2) = 119.16(13), N(2)−Ni(1)−Br(1) = 102.79(15), N(1)−Ni(1)−Br(1) = 125.10(14), Br(2)−Ni(1)−Br(1) = 110.16(4), P(1)−N(1)−Ni(1) = 129.6(2).

Scheme 2

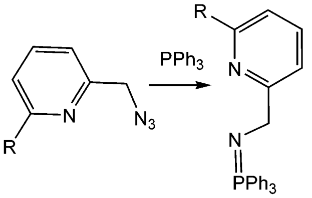

distances in the complex [(CH$_2$(Ph$_2$PN(4-MeC$_6$H$_4$)$_2$Rh-(COD)].[14] The NPCNM five-membered chelate rings are distorted from planar orientations. Atom displacements from the mean planes are relatively small, with the maximum being 0.1026 Å for **40**. Such distortions arise presumably to minimize steric interactions of the pyridine substituents with the metal center.

Pyridine−Phosphinimine (Exocyclic P) Ligand Complexes. A second strategy to related pyridine−phosphinimine ligands involved the use of a series of 2-(azidomethyl)pyridines, which were prepared from known precursors. These compounds were then used to oxidize PPh$_3$, affording the ligands 2-(Ph$_3$PNCH$_2$)-(C$_5$H$_4$N) (**44**), 2-(Ph$_3$PNCH$_2$)-6-Me(C$_5$H$_3$N) (**45**), and 2-(Ph$_3$PNCH$_2$)-6-Ph(C$_5$H$_3$N) (**46**) in yields ranging from 55 to 86% (Scheme 2). The NMR spectra of **44**−**46** showed the expected ^{1}H resonances, and the ^{31}P signals were all approximately 7.8 ppm.

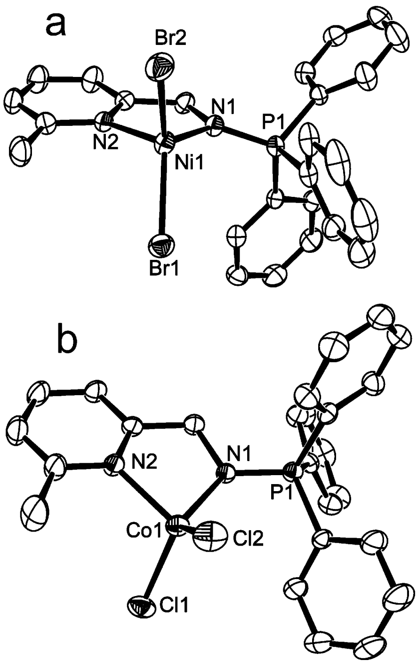

Figure 7. ORTEP drawings of (a) **50** and (b) **54**, with 30% thermal ellipsoids. Hydrogen atoms have been omitted for clarity. Bond lengths (Å) and angles (deg) for **50**: Ni(1)−N(1) = 1.983(3), Ni(1)−N(2) = 2.008(3), Ni(1)−Br(1) = 2.3825(12), Ni(1)−Br(2) = 2.3875(11), P(1)−N(1) = 1.609(3); N(1)−Ni(1)−N(2) = 84.13(11), N(1)−Ni(1)−Br(1) = 113.72(9), N(2)−Ni(1)−Br(1) = 111.91(9), N(1)−Ni(1)−Br(2) = 115.90(9), N(2)−Ni(1)−Br(2) = 104.98(9), Br(1)−Ni(1)−Br(2) = 119.82(3), P(1)−N(1)−Ni(1) = 128.28(16). Bond distances (Å) and angles (deg) for **54**: Co(1)−N(1) = 1.989(2), Co(1)−N(2) = 2.053(2), Co(1)−Cl(2) = 2.2327(11), Co(1)−Cl(1) = 2.2663(12), N(1)−C7 = 1.471(3), N(1)−P(1) = 1.601(2); N(1)−Co(1)−N(2) = 83.72(9), N(1)−Co(1)−Cl(2) = 113.19(7), N(2)−Co(1)−Cl(2) = 116.99(8), N(1)−Co(1)−Cl(1) = 120.52(7), N(2)−Co(1)−Cl(1) = 103.51(7), Cl(2)−Co(1)−Cl(1) = 114.70(4), P(1)−N(1)−Co(1) = 128.72(12).

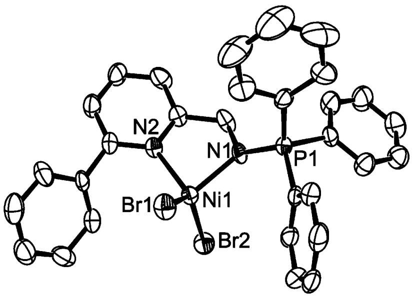

Figure 8. ORTEP drawing of one of the two molecules of **51** in the asymmetric unit, with 30% thermal ellipsoids. Hydrogen atoms have been omitted for clarity. Bond lengths (Å) and angles (deg): Ni(1)−N(2) = 2.008(10), Ni(1)−N(1) = 2.007(10), Ni(1)−Br(1) = 2.363(2), Ni(1)−Br(2) = 2.417(2), P(1)−N(1) = 1.572(10); N(2)−Ni(1)−N(1) = 85.2(4), N(2)−Ni(1)−Br(1) = 106.4(3), N(1)−Ni(1)−Br(1) = 113.0(3), N(2)−Ni(1)−Br(2) = 107.4(3), N(1)−Ni(1)−Br(2) = 102.0(3), Br(1)−Ni(1)−Br(2) = 132.58(9), N(1)−P(1)−C(13) = 114.8(6), P(1)−N(1)−Ni(1) = 131.6(7).

By methods similar to those described above, a series of metal complexes of these pyridine−phosphinimine ligands with exocyclic phosphine groups were prepared. Complexes of (L)PdCl$_2$ (**47**, **48**; L = **44**, **45**) were prepared and characterized spectroscopically. As was the case for **20**, ^{1}H NMR data revealed minor changes while the ^{31}P NMR spectrum revealed a substantial shift upon coordination to the metal center. Similarly, the Ni, Fe, and Co complexes (L)NiBr$_2$ (**49**−**51**; L = **44**−**46**), (L)FeCl$_2$ (**52**, **53**; L = **44**, **45**), and (L)CoCl$_2$ (**54**, **55**; L = **44**, **45**) were prepared. X-ray structural data were obtained for the pseudo-tetrahedral compounds **49**−**51** and **54** (Figures 6−8). For the Ni complex **49**, the Ni−Br distances are similar to those above, all ranging from 2.3611(16) to 2.417(2) Å. The P−N bond lengths in **49**−**51** ranged from 1.572(10) to 1.615(5) Å, which are also similar to those found in **20**, **26**, **27**, **35**, **37**, and **40**. In contrast to the endocyclic P-ligand complexes, these species exhibit Ni−N$_{py}$ and Ni−N$_{Phos}$ bond lengths

---

(46) Tolmachev, A. A.; Yurchenko, A. A.; Semenova, M. G.; Feshchenko, N. G. *Zh. Obshch. Khim.* **1993**, *63*, 714−716.

Scheme 3

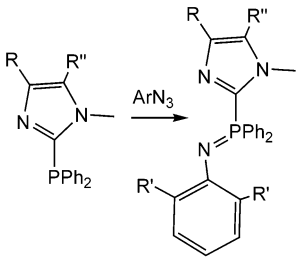

that are very similar (**49**, 1.976(5), 1.977(4) Å; **50**, 1.983(3), 2.008(3) Å; **51**, 2.008(10), 2.007(10) Å). In addition, the Co analogue of **50**, **54**, was also characterized. The geometry of this species is indeed similar to that of the Ni species, with average Co−Cl distances of 2.2545(13) Å and Co−N_{phos} and Co−N_{py} distances of 1.989(2) and 2.053(2) Å, respectively. These structural data reveal that both the electronic and steric changes to the ligand geometry of these ligands with exocyclic phosphine fragments appear to reduce steric congestion at the metal center, allowing strong interactions with the donor atoms. In the case of **51** in particular, we note that the angle between the planes of the pyridine ring and the phenyl substituent is 45.3°. This substituent, together with the exocyclic phosphine group, appears to create a “protective pocket” for the metal center, a feature that augurs well for applications in catalysis.

Imidazole−Phosphinimine Ligand Complexes. Of the known methods for the synthesis of imidazolyl−phosphines,[44−46] the most convenient route involves the selective lithiation of the C2 position of the imidazole followed by reaction with PPh_2Cl. In this manner, the imidazolyl−phosphines 2-(PPh_2)$C_3H_3N_2$ (**56**),[28] 1-Me-2-(PPh_2)-4-(*t*-Bu)C_3HN_2 (**57**),[47,48] 1-Me-2-(PPh_2)$C_3H_2N_2$ (**58**), 1-Me-2-(PPh_2)-4,5-$Ph_2C_3N_2$ (**59**) and 1-Me-2-(PPh_2)-$C_7H_6N_2$ (**60**) were synthesized and isolated in greater than 75% yield. ^{31}P NMR spectroscopy reveals chemical shifts for these species between −25 and −30 ppm. Subsequent oxidation with substituted phenyl azides provides imidazolyl−phosphinimine ligands in excellent yields after recrystallization (Scheme 3). ^1H and ^{31}P NMR spectroscopy were consistent with these formulations, and IR data revealed the typical PN stretching frequencies in the range of 1352−1377 cm^{-1}.

The reaction between compound **62** and $(PhCN)_2PdCl_2$ proceeds to form (1-Me-2-(2,6-*i*-$Pr_2C_6H_3NPPh_2$)($C_3H_2N_2$))-$PdCl_2$ (**68**). ^{31}P NMR spectroscopy shows a singlet at 28.2 ppm, consistent with the expected downfield coordination shift. ^1H NMR spectrum of **68** showed small chemical shift differences compared to the free ligand, with the exception of the observation of two resonances attributable to chemically inequivalent isopropyl methyl groups. Similarly, these methyl groups give rise to inequivalent ^{13}C NMR resonances at 22.5 and 25.1 ppm. Similar observations have been made in related Pd−diimine complexes reported by Brookhart.[4,5]

The X-ray structure of **68** reveals that the imidazole−phosphinimine ligand coordinates in a bidentate fashion with a pseudo-square-planar geometry at Pd (Figure 9).

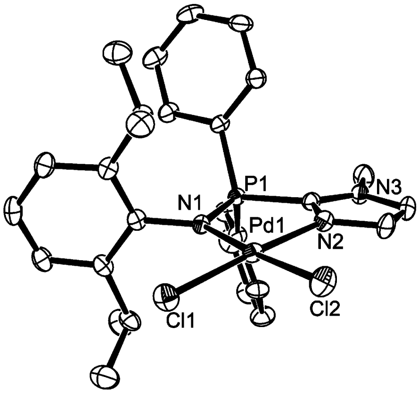

Figure 9. ORTEP drawing of one of the two molecules of **68** in the asymmetric unit, with 30% thermal ellipsoids. Hydrogen atoms have been omitted for clarity. Bond lengths (Å) and angles (deg): Pd(1)−N(2) = 2.026(4), Pd(1)−N(1) = 2.086(4), Pd(1)−Cl(1) = 2.297(2), Pd(1)−Cl(2) = 2.2987(17), P(1)−N(1) = 1.614(4); N(2)−Pd(1)−N(1) = 84.69(14), N(2)−Pd(1)−Cl(1) = 175.56(11), N(1)−Pd(1)−Cl(1) = 93.75(11), N(2)−Pd(1)−Cl(2) = 90.91(11), N(1)−Pd(1)−Cl(2) = 175.33(11), Cl(1)−Pd(1)−Cl(2) = 90.75(5), P(1)−N(1)−Pd(1) = 117.01(19).

In contrast to the pyridine based ligand systems the Pd−N_{Phos} bond length of 2.026(4) Å is slightly shorter than the Pd−N_{Imid} length of 2.086(4) Å. However, the Pd−Cl distances are similar at 2.297(2) and 2.2987(17) Å. The five-membered chelate ring is almost planar, with an average deviation from the mean plane of 0.0178 Å. The P−N bond length in **68** of 1.614(4) Å is longer than that seen in **20** (1.578(3) Å), suggesting that presence of the imidazole fragment also has an electronic effect on the phosphinimine fragment.

Fe(II) and Ni(II) complexes of these imidazole−phosphinimine ligands were synthesized, affording compounds **69**−**75** and **76**−**82**, respectively. These paramagnetic complexes were not soluble in common organic solvents. IR spectroscopy of **69**−**82** showed typical PN stretching frequencies between 1190 and 1250 cm^{-1}, while the magnetic susceptibility measurements of the Ni and Fe complexes of 3.12 and 5.09 μ_B, respectively, were also typical of pseudo-tetrahedral Ni(II) and Fe(II).

X-ray structural determinations of **79** and **82** (Figure 10) confirmed pseudo-tetrahedral geometries with two Cl atoms and the bidentate imidazole−phosphinimine ligand completing the coordination sphere. The Fe−Cl distances in **79** (2.2590(17), 2.2845(15) Å) and **82** (2.2532(14), 2.2790(11) Å) are markedly shorter than those found in **35** but similar to those found in **37** and **40**. The difference in the two types of Fe−N bonds was found to be relatively small (**79**, Fe−N_{Phos} = 2.104(3) Å, Fe−N_{Imid} = 2.114(4) Å; **82**, Fe−N_{Phos} = 2.097(2) Å, Fe−N_{Imid} = 2.140(2) Å) compared to that in the pyridine−phosphinimine complexes above. This suggests that the donors in imidazole−phosphinimine ligands are electronically similar to those in the pyridine−phosphinimine analogues. The P−N distances in both **79** and **82** were similar, averaging 1.599(3) Å, typical of P−N bond lengths in such compounds. The phenyl substituents in **79** are canted at an angle of 49.1° with respect to the imidazole ring, similar to that observed for the phenyl substituent in **40**. The presence of this phenyl ring in **79** or the *t*-Bu group in **82** in the 4-position also

---

(47) Lipshutz, B. H.; Morey, M. C. *J. Org. Chem.* **1983**, *48*, 3745−3750.

(48) Hilf, C.; Bosold, F.; Harms, K.; Lohrenz, J. C. W.; Marsch, M.; Schimeczek, M.; Boche, G. *Chem. Ber.* **1997**, *130*, 1201−1212.

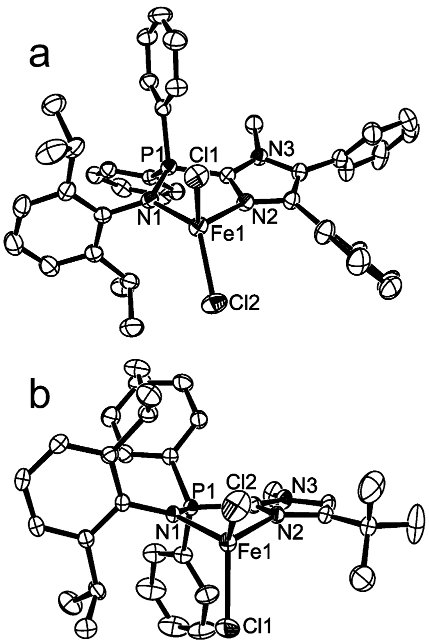

Figure 10. ORTEP drawings of (a) **79** and (b) **82**, in the asymmetric unit, with 30% thermal ellipsoids. Hydrogen atoms have been omitted for clarity. Bond lengths (Å) and angles (deg) for **79**: Fe(1)−N(1) = 2.104(3), Fe(1)−N(2) = 2.114(4), Fe(1)−Cl(2) = 2.2590(17), Fe(1)−Cl(1) = 2.2845(15), P(1)−N(1) = 1.600(3); N(1)−Fe(1)−N(2) = 84.76(12), N(1)−Fe(1)−Cl(2) = 127.04(10), N(2)−Fe(1)−Cl(2) = 108.12(9), N(1)−Fe(1)−Cl(1) = 105.14(10), N(2)−Fe(1)−Cl(1) = 110.33(10), Cl(2)−Fe(1)−Cl(1) = 116.49(6), P(1)−N(1)−Fe(1) = 115.89(18). Bond distances (Å) and angles (deg) for **82**: Fe(1)−N(1) = 2.097(2), Fe(1)−N(2) = 2.140(2), Fe(1)−Cl(1) = 2.2790(11), Fe(1)−Cl(2) = 2.2532(14), N(1)−P(1) = 1.598(2); N(1)−Fe(1)−N(2) = 85.07(7), N(1)−Fe(1)−Cl(2) = 117.48(6), N(2)−Fe(1)−Cl(2) = 115.53(6), N(1)−Fe(1)−Cl(1) = 109.92(7), N(2)−Fe(1)−Cl(1) = 109.31(6), Cl(2)−Fe(1)−Cl(1) = 115.60(4), P(1)−N(1)−Fe(1) = 114.61(10).

Table 3. Ethylene Dimerization

precatalyst	solvent	C_4 oligomer (g)[c]	activity[d]	$1\text{-}C_4H_8$:$2\text{-}C_4H_8$
30[a]	MeC_6H_5	0.807	16.1	1:99
30[b]	ClC_6H_5	7.95	48.2	1:99
40[a]	MeC_6H_5	0.66	13.2	1:99
40[b]	ClC_6H_5	0.50	3.0	1:99
74	MeC_6H_5	0.52	10.3	1:99
74	ClC_6H_5	2.98	17.9	86:13
82	MeC_6H_5	0.10	2.0	1:99
82	ClC_6H_5	0.35	2.1	1:99

[a] Conditions: 300 psig of ethylene, 35 °C, Al:M ratio of 500:1, MAO. [b] Conditions: 300 psig of ethylene, 35 °C, Et_2AlCl, Al:M ratio of 200:1. [c] Calculated from GC and NMR data. [d] In units of g of oligomer (g of cat.)$^{-1}$ h^{-1} atm^{-1}.

forms what appears to be a protected pocket around the metal center similar to those seen in the substituted pyridine−phosphinimine ligand complexes above.

Ethylene Oligomerization. Complexes **27**−**30**, **37**−**40**, **74**, **75**, and **82** were initially screened for activity as catalyst precursors for ethylene polymerization. A 500 equiv amount of MAO or MMAO was employed as the activator in either toluene or hexane at 35 °C under 300 psi of ethylene in a Parr high-pressure reactor. In general, these tests yield no isolable polymer; however, in the case of MMAO activation of **74**, polyethylene of molecular weight 23 100 (PDI 1.34) was obtained. In this case, although the PDI implies a single-site catalyst, the activity of the catalyst was low (3.6 g of PE (mmol of cat.)$^{-1}$ h^{-1} atm^{-1}). In several cases some ethylene consumption was evident, suggesting that ethylene oligomerization may be occurring. On the basis of the findings in related late-metal catalyst systems, the complexes with increased steric bulk adjacent to the metal center, **30**, **40**, **74**, and **82**, were examined in further detail. In these cases, the catalyst was generated in situ via activation with either MAO (toluene) or Et_2AlCl (ClC_6H_5) at 35 °C under 300 psi of ethylene. Under these reaction conditions, these compounds yielded only modest catalytic activity. In general, the Fe(II) complexes exhibited lower activity than the Ni analogues. Of these, the Ni catalyst generated from **30**/Et_2AlCl gave the highest activity (Table 3). GC and NMR data confirmed the products were 1- and 2-butenes, 2-butene being the major product in most cases. Only for **74** in chlorobenzene did NMR and GC analysis show 1-butene as the predominant product, with minor amounts of *cis*- and *trans*-butene. The reason for the reversal in selectivity is unclear, although the selective production of 1-butene is similar to that observed by Sun et al. for a P,N-chelated Ni catalyst.[49] Nonetheless, it is noteworthy that the present systems exhibited much lower dimerization activity. Similarly, catalysts derived from Ni−bis(phosphinimine) complexes and Et_2AlCl produced primarily C_4 alkenes with smaller amounts of C_6 and C_8 alkenes,[18] although those catalysts as well as other known dimerization and oligomerization catalysts[2] exhibited significantly higher activity than the present systems.

Computation and Ligand Considerations. On the basis of DFT studies of cationic nickel−diimine complexes[50−59] Tomita et al. have suggested that σ-donation of ethylene participates in the coordinate nickel bond to a greater extent than π-back-donation[59] and that the degree of σ-donation by ethylene will be influenced by the trans-coordinated ligand. Furthermore, the energy of the lone pair of electrons on the trans-donor ligand reflects its trans influence; thus, the greater the energy of the lone pair orbital, the more electron donating the ligand is to the metal center. DFT calculations of the orbital energies for the ligand models of HNCHCHNH, $HNPH_2CHNH$, and $HNCHCH_2NPH_3$ (Chart 1) showed that HOMO-1 and the HOMO-2 correspond to the lone pairs of the imine and phosphinimine fragments, respectively. The results (Table 4) indicate that the presence of a P atom in the ligand backbone increases

---

(49) Sun, W.-H.; Li, Z.; Hu, H.; Wu, B.; Yang, H.; Zhu, N.; Leng, X.; Wang, H. *New J. Chem.* **2002**, *26*, 1474−1478.

(50) Chan, M. S. W.; Deng, L.; Ziegler, T. *Organometallics* **2000**, *19*, 2741−2750.

(51) Fan, L.; Krzywicki, A.; Somogyvari, A.; Ziegler, T. *Inorg. Chem.* **1994**, *33*, 5287−5294.

(52) Fan, L.; Krzywicki, A.; Somogyvari, A.; Ziegler, T. *Inorg. Chem.* **1996**, *35*, 4003−4006.

(53) Margl, P.; Ziegler, T. *J. Am. Chem. Soc.* **1996**, *118*, 7337−7344.

(54) Deng, L.; Margl, P.; Ziegler, T. *J. Am. Chem. Soc.* **1997**, *119*, 1094−1100.

(55) Deng, L.; Woo, T. K.; Cavallo, L.; Margl, P. M.; Ziegler, T. *J. Am. Chem. Soc.* **1997**, *119*, 6177−6186.

(56) Woo, T. K.; Bloechl, P. E.; Ziegler, T. *J. Phys. Chem.* **2000**, *104*, 121−129.

(57) Musaev, D. G.; Froese, R. D. J.; Morokuma, K. *New J. Chem.* **1997**, *21*, 1269−1282.

(58) Musaev, D. G.; Froese, R. D. J.; Svensson, M.; Morokuma, K. *J. Am. Chem. Soc.* **1997**, *119*, 367−374.

(59) Tomita, T.; Takahama, T.; Sugimoto, M.; Sakaki, S. *Organometallics* **2002**, *21*, 4138−4146.

Chart 1

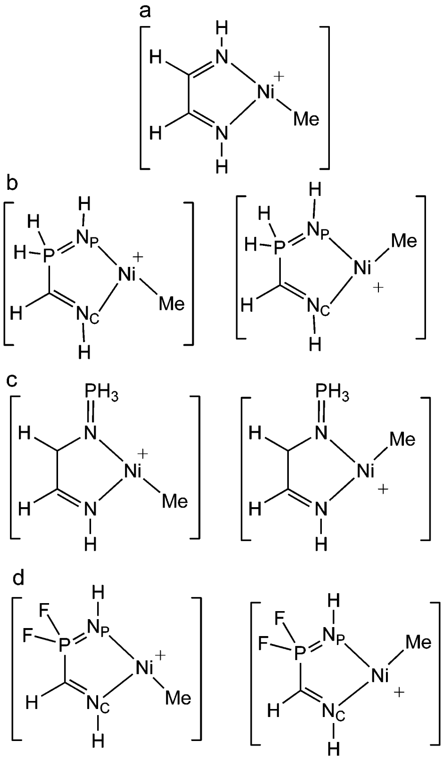

Table 4. DFT Calculations: Ligand Lone Pair Energies[a] and Atomic Charges on Ni

	HNCH-CHNH	$HNPH_2$-CHNH	HNCHC-H_2NPH_3	$HNPF_2C$-HNH
$E_{\text{lone pair}}(N_C)$ (HOMO-2)	−11.6;[c] −11.3[d]	−11.5	−10.7	−12.5
$E_{\text{lone pair}}(N_P)$ (HOMO-1)	-	−9.2	−9.8	−11.2
sym of N[(L)NiMe]$^+$	C_s	C_1	C_1	C_1
[(L)NiMe]$^+$ [b]	0.858	0.832;[e] 0.816[f]	0.809;[e] 0.830[f]	0.856;[e] 0.861[f]

[a] Energies measured in eV. [b] NBO charge of Ni. [c] Antibonding combination of lone pairs. [d] Bonding combination of lone pairs. [e] NBO of Ni with CN cis to Ni−Me. [f] NBO of Ni with PN cis to Ni−Me.

the lone-pair energies for both N-atom donors. This is also consistent with NBO analysis of the models of [(L)NiMe]$^+$, which showed that the $HNCHCH_2NPH_3$ complex exhibited a lower positive charge on Ni (Table 4). This suggests that regardless of which site the ethylene ligand occupies in the cationic Ni complex [($HNCHCH_2NPH_3$)NiMe(CH_2CH_2)]$^+$, the M−ethylene interaction is expected to be weaker than in the diimine analogue. Furthermore, a lower charge on Ni inhibits charge transfer from the ethylene C−H bonding orbital to the empty d orbital, thus also leading to a weaker agostic interaction between Ni and ethylene. This may account for the observation of slow dimerization rather than polymerization of ethylene. F atom substituents on P in the model $HNPF_2CHNH$ resulted in a discernible decrease in lone pair energy and increase in the charge on Ni, suggesting that the presence of electron-withdrawing substituents on P could improve the M−ethylene interactions. Unfortunately, efforts to put this into practice by the incorporation of C_6F_5 substituents were unsuccessful, as the corresponding pyridine−phosphine **6** could not be oxidized with aryl azides.

Summary

We have developed synthetic methods for three classes of dissymmetric phosphinimine chelate ligands. Fe and Ni complexes of such ligands, upon activation, yielded only modest activity for the dimerization of ethylene. DFT computations infer that inclusion of P into the ligand results in diminished electrophilicity at Ni and thus a weakened ethylene−metal interaction. Efforts to introduce electron-withdrawing groups on the P atom to explore other applications of these complexes and to explore the utility of other ligand systems in ethylene oligomerization are currently underway.

Acknowledgment. Financial support from the NSERC of Canada and NOVA Chemicals Corp. is gratefully acknowledged. L.P.S. is grateful for the award of an Ontario Graduate Scholarship, and R.A. is grateful for support from the Waha Oil Co. D.W.S. is grateful for the award of Forschungpreis from the Alexander von Humboldt Stiftung.

Supporting Information Available: Crystallographic data for all structures reported herein, as CIF files, and figures giving ^{1}H NMR spectra of all ligands and ligand precursors. This material is available free of charge via the Internet at http://pubs.acs.org.

OM030311T